



**Drug Repurposing for Colorectal Cancer: In Silico Identification  
of Pazopanib and Brequinar as Potential Therapeutics Targeting  
Oncogenic Pathways**

**A project submitted to the  
Department of Bioinformatics**

**Dr. D. Y. Patil Arts, Commerce & Science College, Pimpri, Pune-18**

**Affiliated to Savitribai Phule Pune, University, Pune, Maharashtra**

**For the degree of  
M. Sc. In Bioinformatics**

**By  
Shouryan Jivraj Patil**

**Under the Guidance of  
Prof. Shraddha Ranpise**

**HOD,  
Department of Bioinformatics, Dr. D. Y. Patil Arts, Commerce and Science College,  
Pimpri, Pune-18**

**June, 2025**

## DECLARATION & UNDERTAKING

I hereby declare that the project entitled, “Drug Repurposing for Colorectal Cancer: In Silico Identification of Pazopanib and Brequinar as Potential Therapeutics Targeting Oncogenic Pathways”, submitted in partial fulfilment of the requirements of the degree of Master of Science in Bioinformatics, has been carried out by me at Department of Bioinformatics, Dr. D. Y. Patil Arts, Commerce and Science College, Pimpri, Pune-18 under the guidance of Prof. Shraddha Ranpise.

I further declare that the project work or any part thereof has not been previously submitted for any degree or diploma of any University. I also declare that to the best of my ability, I have ensured that the submission made herein, including the main text, supplementary data, deposited data, database entries, software code, figures, does not contain any plagiarized material, content or ideas, and that all necessary attributions have been appropriately made and all copyright permissions obtained, cited and acknowledged.

I also declare that any further extension, continuation, publication, patenting or any other use of this project (either in full or in part), if any, shall be undertaken with prior written consent from the Director, Department of Bioinformatics, Dr. D. Y. Patil Arts, Commerce and Science College, Pimpri, Pune-18 and the Project Supervisor/s.

I further state that I shall explicitly mention, “Department of Bioinformatics, Dr. D. Y. Patil Arts, Commerce and Science College, Pimpri, Pune-18” as “Place of Work” and acknowledge the “M.Sc. Bioinformatics” training programme at Department of Bioinformatics, Dr. D. Y. Patil Arts, Commerce and Science College, Pimpri, Pune-18 for infrastructure and facilities” in the publication (print and online)/patent based on this work.

**Date: --/--/--**

**Students' Name: Mr. Shouryan Jivraj Patil**

## **ACKNOWLEDGEMENTS**

I owe my deepest gratitude to my guide, Prof. Shraddha Ranpise, HOD of Department of Bioinformatics, Dr. D. Y. Patil ACS College, Pimpri Pune a wonderful guide throughout the course of my study. I take this opportunity to acknowledge her guidance and encouragement. I express my sincere gratitude for her for bringing me thus far in my career. I have been inspired by her erudite guidance, meticulousness, energetic approach and attention to detail to solve any problem. I value her concern and support at all times. Her scholarly guidance and inspiring suggestions have helped me in carrying out the present research work. She has been a constant source of learning. Her immense knowledge, expert guidance, constructive suggestions helped me improve my research thinking. I whole heartedly thank her for being my guide. I have been privileged to work under her supervision.

I sincerely thank Prof. Pratiksha Bhoi and Prof. Preeti Mate, Assistant Professors at Dr. D. Y. Patil ACS College, Pimpri, Pune, for their continuous support, motivation, and guidance throughout my research work. Their valuable suggestions and encouragement have greatly contributed to the successful completion of my project. The constructive discussions and academic guidance provided by them have been immensely beneficial to me at various stages of my work.

I express my gratitude to Dr. Ranjit Patil, Principal, Dr. D. Y. Patil ACS College Pimpri for his cooperation and support and for permitting me to carry out research work in this esteemed institute. I thank my classmates, non-teaching staff members for their help, encouragement and joyful time shared during the path of this research work.

I am highly indebted to my parents for their unconditional love and encouragement. They have worked for me as a source of emotional strength during this period. Their prayers and blessings have helped me to come this far... Last but by no means least, I acknowledge above all I thank the ALMIGHTY GOD, who is always with me and showers his blessings and grace towards me in all walks of my life.

**Shouryan Jivraj Patil**

## **TABLE OF CONTENTS**

• Abstract	V
• List Of Abbreviations	VI
• List of Tables	VII
• List of Figures	VIII
1. Introduction	10
2. Materials and Methods	16
3. Results and Discussions	25
4. Conclusion	50
5. Future Work	52
6. References	53

## ABSTRACT

Colorectal cancer (CRC) remains a significant global health challenge as the second deadliest and third most diagnosed cancer, with its incidence projected to double by 2035, particularly in less developed regions. Current therapeutic options are limited by complex disease progression, treatment resistance, and the inefficiencies of traditional drug development, which is costly and time-intensive with low success rates. This study explores drug repurposing as a promising alternative to identify effective CRC treatments by targeting key oncogenic pathways, including EGFR/MAPK, Wnt/ $\beta$ -catenin, and PI3K/AKT. Using in silico methods, we screened FDA-approved drugs for their potential to inhibit critical CRC-related proteins. Molecular docking revealed Pazopanib and Brequinar as top candidates, exhibiting strong binding affinities to PI3K (-11.72 kcal/mol and -9.62 kcal/mol, respectively) and MEK (-10.94 kcal/mol and -8.77 kcal/mol, respectively), outperforming some standard CRC drugs like Regorafenib. Molecular dynamics simulations confirmed Brequinar's superior stability with PI3K and KRAS, while ADMET analysis highlighted its favorable pharmacokinetic profile despite high plasma protein binding. These findings suggest that repurposing Pazopanib and Brequinar could offer a faster, cost-effective, and lower-risk approach to CRC therapy. Further in vitro and in vivo validation is needed to translate these findings into clinical applications and accelerate CRC treatment development.

## LIST OF ABBREVIATIONS

ADMET	Absorption, Distribution, Metabolism, Excretion, and Toxicity
APC	Adenomatous Polyposis Coli
BBB	Blood-Brain Barrier
CIN	Chromosomal Instability
CRC	Colorectal Cancer
EGFR	Epidermal Growth Factor Receptor
FDA	Food and Drug Administration
GSK-3 $\beta$	Glycogen Synthase Kinase-3 Beta
KRAS	Kirsten Rat Sarcoma Viral Oncogene Homolog
MAPK	Mitogen-Activated Protein Kinase
MD	Molecular Dynamics
MEK	Mitogen-Activated Protein Kinase Kinase
mTOR	Mammalian Target of Rapamycin
NF- $\kappa$ B	Nuclear Factor Kappa B
NPT	Constant Number, Pressure, and Temperature (ensemble)
NVT	Constant Number, Volume, and Temperature (ensemble)
PDB	Protein Data Bank
PI3K	Phosphoinositide 3-Kinase
PTEN	Phosphatase and Tensin Homolog
RMSD	Root Mean Square Deviation
RMSF	Root Mean Square Fluctuation
RoG	Radius of Gyration
TKI	Tyrosine Kinase Inhibitor
TGF- $\beta$	Transforming Growth Factor Beta

## LIST OF TABLES

Title	Page No
Table I: Selected Target Proteins from Key Colorectal Cancer Pathways with Corresponding PDB IDs	17
Table II: Selection of Ligands Based on Similarity to Approved CRC Drugs	19
Table III: Active Site Coordinates of Selected Target Proteins	26
Table IV: Insilico Docking score of the Compound	27
Table V: Insilico Docking score of the Compound	28
Table VI: Structural properties of the Compound	33
Table VII: Structural properties of the Compound	33
Table VIII: Absorption of the Compound	34
Table IX: Absorption of the Compound	34
Table X: Distribution of the Compound	34
Table XI: Distribution of the Compound	35
Table XII: Metabolism of the Compound	35
Table XIII: Metabolism of the Compound	36
Table XIV: Excretion of the Compound	36
Table XV: Excretion of the Compound	37
Table XVI: Toxicity of the Compound	37
Table XVII: Toxicity of the Compound	38

## LIST OF FIGURES

Title	Page No
Fig.1 Progression of Colorectal Cancer from Normal Colon Tissue	12
Fig.2: 3D structure of EGFR	25
Fig.3: 3D structure of KRAS	25
Fig.4: 3D structure of BRAF	25
Fig.5: 3D structure of PIK3CA	25
Fig.6: 3D structure of MEK	25
Fig.7: 3D structure of ERK1	25
Fig.8: 3D structure of $\beta$ -Catenin	25
Fig.9: 3D structure of GSK-3 $\beta$	25
Fig.10: 3D structure of APC	25
Fig.11: 3D structure of PI3K	25
Fig.12: 3D structure of AKT	25
Fig.13: 3D structure of mTOR	25
Fig.14: 3D structure of GREM1	25
Fig.15: 3D structure of CSF2RA	25
Fig.16: 2D structure of Adagrasib	27
Fig.17: 2D structure of Regorafenib	27
Fig.18: 2D structure of Trifluridine	27
Fig.19: 2D structure of Benzimidazole	27
Fig.20: 2D structure of Pyrimidine	27
Fig.21: 2D structure of Pazopanib	27



Fig.22: 2D structure of Tivozanib	27
Fig.23: 2D structure of Fludarabine	27
Fig.24: 2D structure of Vidarabine	27
Fig.25: 2D structure of Brequinar	27
Fig. 26: Heatmap Representation of Molecular Docking Binding Energies	29
Fig. 27: 3D and 2D structure of Pazopanib with PI3K	30
Fig. 28: 3D and 2D structure of Pazopanib with MEK	30
Fig. 29: 3D and 2D structure of Pazopanib with ERK1	31
Fig. 30: 3D and 2D structure of Brequinar with PI3K	31
Fig. 31: 3D and 2D structure of Brequinar with EGFR	32
Fig. 32: 3D and 2D structure of Brequinar with KRAS	32
Fig.33: RMSD graph of PI3K with Pazopanib, Brequinar and Regorafenib	39
Fig.34: RMSD graph of EGFR with Brequinar and Regorafenib	40
Fig.35: RMSD graph of KRAS with Brequinar and Regorafenib	41
Fig.36: RMSF graph of PI3K with Pazopanib, Brequinar and Regorafenib	42
Fig.37: RMSF graph of EGFR with Brequinar and Regorafenib	43
Fig.38: RMSF graph of KRAS with Brequinar and Regorafenib	44
Fig.39: RoG graph of PI3K with Pazopanib, Brequinar and Regorafenib	45
Fig.40: RoG graph of EGFR with Brequinar and Regorafenib	46
Fig.41: RoG graph of KRAS with Brequinar and Regorafenib	47

# 1. INTRODUCTION

Colorectal cancer (CRC), which includes colon and/or rectal cancer, is the second most deadly and third most frequently diagnosed cancer worldwide, making it a serious health issue (WHO 2025). In 2020, colorectal cancer accounted for about 9.4% of all cancer-related deaths (Ferlay et al., 2025). However, it is predicted that the global incidence of colorectal cancer (CRC) would more than double by 2035 due to the notable rise in the number of cases found in the elderly population, with less developed countries experiencing the largest increase (Papamichael et al., 2015).

The traditional cancer model proposed that a normal cell changes into an atypical or dysplastic cell, eventually evolving into an invasive or malignant cell (Idikio, 2011). Cancer can be described as the uncontrolled growth and division of cells. Cancer cells have the ability to disseminate and invade different areas of the body via the bloodstream and lymphatic system (Hanahan & Weinberg, 2000). At the cellular level, cancer typically arises through three distinct phases: Initiation, promotion, and progression. The initial phase, initiation, takes place when genetic, metabolic, and carcinogenic elements cause harm to the DNA molecule (Cooper 2000; Doll & Peto, 1981). Carcinogens such as radiation, chemicals, and viruses have been shown to cause cancer in both laboratory animals and humans (Cooper, 2000; Blackadar, 2016). Carcinogens function by harming DNA and causing mutations (Cooper, 2000) through a mechanism known as carcinogenesis, which includes the activation of oncogenes and/or the suppression of tumor suppressor genes, resulting in unregulated cell cycle progression and the inhibition of apoptosis (Sarkar et al., 2013). The promotion phase is the second stage of cancer development. This is an extended phase that starts with the multiplication of cells that become abnormal during the initiation phase. Progression is the third and last stage, characterized as the metastasis of tumor cells that form during the proliferation phase (Doll & Peto, 1981). However, a single genetic mutation alone is inadequate to cause cancer progression; thus, the multiple-hit hypothesis suggests that cancer arises from the accumulation of genetic mutations within a cell's DNA. This suggested hypothesis was initially documented by Nordling (1953) and subsequently by Knudson (1971) and Centelles (2012).

The word 'tumor' refers to the unusual growth of cells and can be classified as either benign or malignant. The difference between benign and malignant tumors is the key concern in cancer pathology (Cooper, 2000). The features that distinguish malignant from benign lesions are clearly defined and include a fast growth rate, heightened cell turnover, invasive growth,

metastasis, and invasion of lymphatic and/or vascular channels (Idikio, 2011; Van Raamsdonk et al., 2009). Benign tumors stay localized to their initial site, without encroaching on nearby normal tissues or spreading to distant areas (Cooper, 2000). Nevertheless, cancerous tumors have the ability to invade adjacent healthy tissues and disseminate (metastasize) to different areas of the body through the blood or lymphatic systems (Cooper, 2000; Sarkar et al., 2013). Only malignant tumors are categorized as cancers, and their potential to metastasize is what renders cancer perilous. The dissemination of malignant tumors to remote areas in the body often leads to their resistance to therapy (Cooper, 2000).

### **1.1 Colorectal Cancer Development**

CRC is a condition that happens only in the colon or rectum and is brought about by the abnormal growth of glandular epithelial cells in the colon. There are three main categories of CRC: Sporadic, hereditary, and colitis-related. The global incidence of CRC cases is rising every day. The risk of developing CRC is influenced by both genetic and environmental factors. Moreover, the likelihood of developing CRC in individuals with chronic ulcerative colitis and Crohn's disease rises as they get older (Triantafyllidis et al., 2009). Numerous studies have shown that risk factors for CRC encompass diet and lifestyle, family background, and persistent inflammation. However, the most efficient way to avert CRC and decrease CRC-related fatalities in the population is by screening those at average risk (Edwards et al., 2010). Furthermore, population-centric screening seeks to uncover hidden diseases within the average-risk group, facilitating early interventions and diminishing risks for individuals and/or communities (Wilson & Jungner, 1968). The development of CRC spans several years. Typically, a polyp takes 10 to 15 years to develop into a malignant tumor. Therefore, regular screening, identifying, and eliminating polyps in the initial phase is essential; thus, CRC can be avoided. Present diagnostic methods can identify only 40% of CRC cases during the early phases, and CRC can reoccur after surgical procedures and subsequent treatment (ACS, 2020).

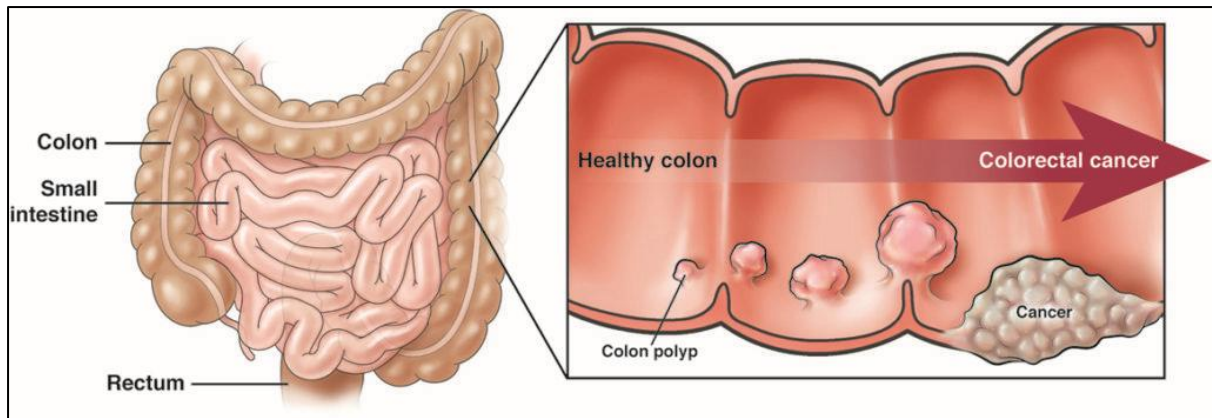


Fig.1 Progression of Colorectal Cancer from Normal Colon Tissue

CRC arises when epithelial cells undergo a sequence of genetic or epigenetic alterations that allow them to become hyperproliferative (Testa et al., 2018). These quickly evolving cells create a benign adenoma, which can progress to cancer and spread through various unique pathways, such as microsatellite instability (MSI), chromosomal instability (CIN), and serrated neoplasia (Malki et al., 2020; Bian et al., 2020; Vogelstein et al., 1988). The adenoma–carcinoma sequence refers to the process of cancer development. The conventional route accounts for a significant number of sporadic CRC instances. Cancer starts as a small adenoma, grows into a large adenoma, and ultimately develops into cancer. A significant link exists between this pathway and the emergence of the chromosomal instability (CIN)-positive subtype (CIN-positive). The National Cancer Institute states that this model represents 10–15% of sporadic CRC. It is characterized by progression from normal cells to hyperplastic polyps, sessile serrated adenomas, and ultimately cancer (Keum & Giovannucci, 2019). Since it takes years for cancer to develop, there is a chance for secondary prevention of colorectal cancer. The development of CRC is a complex, multi-phase process that entails sequential mutations. Multiple cellular signaling pathways involved in regulating cell growth, differentiation, apoptosis, and survival contribute to the initiation of CRC. These include the epidermal growth factor receptor (EGFR)/mitogen-activated protein kinase (MAPK), Wingless-related integration site (Wnt)/ $\beta$ -catenin, phosphoinositide 3-kinase (PI3K), transforming growth factor- $\beta$  (TGF- $\beta$ ), Neurogenic locus notch homolog protein (Notch), and nuclear factor (NF)- $\kappa$ B.

### **1.1.1 EGFR/MAPK Signaling Pathway**

The EGFR/MAPK signaling pathway plays a critical role in colorectal cancer (CRC) by regulating cell proliferation, differentiation, and survival. EGFR, a receptor tyrosine kinase, contains an extracellular ligand-binding domain and undergoes activation and dimerization upon ligand binding, leading to autophosphorylation of tyrosine residues in the intracellular domain. This initiates a signaling cascade through the recruitment of adaptor proteins Grb2 and SOS, which activate RAS by converting GDP to GTP (Ahmad et al., 2021). Activated RAS triggers a kinase cascade involving RAF (MAPKKK), MEK (MAPKK), and ERK (MAPK), ultimately influencing oncogenic gene expression. Dysregulation of this pathway has been implicated in various cancers, including CRC, as it promotes malignant transformation by enhancing cell proliferation, prolonged survival, angiogenesis, anti-apoptosis, invasion, and metastasis (Barbosa et al., 2021). Studies have directly linked the EGFR/MAPK pathway to CRC progression, highlighting its crucial role in tumor growth and disease advancement (Jeong et al., 2018). Given its significance in CRC oncogenesis, this pathway and its downstream signaling components have been explored as therapeutic targets for intervention (Saletti et al., 2015; Malki et al., 2020).

### **1.1.2 Wnt/ $\beta$ -Catenin Pathway**

The Wnt/ $\beta$ -catenin signaling pathway is crucial in developmental processes and carcinogenesis, including cell proliferation, migration, and division. All 19 glycoproteins of the Wnt family regulate various biological functions, such as tissue maintenance and regeneration of hair, skin, and the intestine. Mutations in this pathway are frequently observed in sporadic colorectal cancer (sCRC) (Koveitypour et al., 2019; Świerczyński et al., 2021). Upon Wnt ligand accumulation and binding to Frizzled (Fz) receptors, glycogen synthase kinase-3 $\beta$  (GSK-3 $\beta$ ) is inactivated, leading to the stabilization and nuclear translocation of  $\beta$ -catenin. In the nucleus,  $\beta$ -catenin interacts with lymphoid enhancer factor (LEF) or T-cell transcription factor (TCF) to activate target genes involved in cell proliferation and transmission. In the absence of Wnt signaling,  $\beta$ -catenin is phosphorylated by casein kinase 1 (CK1) and the APC-Axin-GSK-3 $\beta$  complex, marking it for ubiquitination and proteasomal degradation. Hyperactivation of Wnt signaling contributes to tumor cell proliferation and is essential for tumor progression, particularly in advanced CRC stages (Koveitypour et al., 2019; Świerczyński et al., 2021).

### **1.1.3 PI3K Signaling Pathway**

The PI3K signaling pathway plays a critical role in regulating various cellular activities, including growth, proliferation, differentiation, migration, and survival (Narayanankutty, 2019). PI3K is a heterodimeric molecule composed of a regulatory subunit (p85) and a catalytic subunit (p110). Protein kinase B (AKT/PKB), a downstream effector of PI3K, is a serine/threonine kinase that mediates tumor growth and progression (Kaya Temiz et al., 2014). AKT phosphorylation has been implicated in promoting cell proliferation and inhibiting apoptosis in human colorectal cancer (CRC), making the PI3K/AKT pathway a target for cancer treatment (Castel et al., 2021). PI3K is activated upon ligand binding to receptor tyrosine kinases (RTKs), leading to the phosphorylation of phosphatidylinositol 4,5-bisphosphate (PIP2) into phosphatidylinositol 3,4,5-trisphosphate (PIP3). PIP3, in turn, activates AKT by phosphorylating its serine and threonine residues, thereby promoting cell proliferation and survival. AKT further regulates downstream effectors such as the mammalian target of rapamycin (mTOR), which influences cell cycle progression, proliferation, angiogenesis, protein synthesis, and survival. The phosphatase and tensin homolog (PTEN), a tumor suppressor and negative regulator of the PI3K pathway, dephosphorylates PIP3, thereby inhibiting PI3K signaling. In CRC, altered expression of this pathway results in unchecked cell growth and contributes to tumor development. Overall, the PI3K signaling pathway is considered oncogenic and plays a significant role in CRC initiation and progression (Narayanankutty, 2019; Kaya Temiz et al., 2014; Castel et al., 2021).

### **1.2 Significance of Drug Repurposing in Colorectal Cancer**

Drug repurposing, also known as repositioning, refers to the application of existing approved drugs for treating diseases other than their originally intended condition (Giampieri et al., 2020; Jourdan et al., 2020; Nowak-Sliwinska et al., 2019). Over the years, several drugs have gained new therapeutic applications and have been reintroduced into medical practice due to this phenomenon. For example, thalidomide, originally withdrawn as an antiemetic, is now utilized in the treatment of multiple myeloma (Kumar et al., 2020) and moderate to severe erythema nodosum leprosum (Upputuri et al., 2020). Another example is Sildenafil, which preserves both its primary indication for erectile dysfunction (Fink et al., 2002) and its repurposed use as a treatment for idiopathic pulmonary hypertension (Barnett & Machado, 2006). Drug repurposing has re-emerged as an effective, expedited, and relatively safer strategy for drug development. In contrast, the traditional development of new drugs typically takes

around 10–15 years (Institute of Medicine, 2010), with a reported success rate ranging from 2% to 10% (Xue et al., 2018; U.S. Food and Drug Administration, 2025). According to the U.S. Food and Drug Administration (FDA), as of 2018, only about 6% of drug candidates successfully reached stage 4 clinical trials (Deotarse et al., 2015). Drug repurposing significantly reduces development timelines and costs, estimated to be 160 million times lower, particularly in areas such as safety testing, molecular characterization, safety profiling, and initial marketing. By utilizing existing knowledge on genetic, pharmacodynamic, pharmacokinetic, and adverse effect profiles, it often bypasses stage 1 clinical trials (Parvathaneni et al., 2019). Thus, this approach provides a more cost-effective, accelerated, and lower-risk alternative to conventional drug development (Xue et al., 2018).

Colorectal cancer (CRC) poses a significant global health burden, with rising incidence and mortality rates, yet current therapeutic options often fail to address its complex progression and resistance to treatment effectively. The slow pace, high costs, and low success rates of traditional drug development further complicate the search for new solutions, highlighting the need for innovative approaches to improve patient outcomes. This study tackles the research problem of identifying effective treatment alternatives by exploring drug repurposing, with the objectives of discovering existing drugs that can target CRC's molecular mechanisms and assessing their potential efficacy through computational methods. The scope of the study focuses on *in silico* screening and analysis of approved drugs, aiming to uncover candidates that could offer a faster, cost-effective, and lower-risk path to CRC therapy development.

## 2. MATERIALS AND METHODS

### 2.1. Protein Information

Colorectal cancer (CRC) is driven by multiple dysregulated signaling pathways, including the Wnt/ $\beta$ -catenin, PI3K/Akt, EGFR, and MAPK pathways (Li et al., 2024). These pathways play crucial roles in cancer initiation, progression, and therapeutic resistance. To identify potential drug targets for CRC, key proteins involved in these pathways were selected based on their well-documented roles in oncogenesis.

#### 2.1.1 Target Pathway Selection

A literature review was conducted to identify critical signaling pathways implicated in CRC progression. Based on previous studies, four primary pathways were selected due to their involvement in tumor proliferation, survival, and metastasis:

1. **EGFR Pathway** – Regulates cell growth and proliferation through downstream activation of RAS-RAF-MEK-ERK signaling. Overactivation of EGFR is frequently observed in CRC, making it a therapeutic target (Koveitypour et al., 2019).
2. **MAPK Pathway** – Plays a role in cell differentiation, survival, and apoptosis. Dysregulation of this pathway contributes to uncontrolled cell division (Guo et al., 2020).
3. **Wnt/ $\beta$ -Catenin Pathway** – Critical for maintaining stemness and cellular homeostasis; mutations in APC and  $\beta$ -catenin genes are commonly found in CRC (Bian et al., 2020).
4. **PI3K/AKT Pathway** – Regulates cell metabolism, growth, and survival. Aberrant activation of PI3K and AKT promotes cancer cell proliferation (Maharati & Moghbeli, 2023).

To validate the selection, relevant proteins from each pathway were retrieved from the Protein Data Bank (PDB) for structural analysis. The chosen proteins, their roles, and corresponding PDB IDs are presented in Table I.

#### 2.1.2 Selection of Target Proteins

The following proteins were selected for further computational analysis based on their involvement in key CRC pathways:



Table I: Selected Target Proteins from Key Colorectal Cancer Pathways with Corresponding PDB IDs

Pathway	Sr. No.	Protein Name	PDB ID
<b>EGFR Pathway</b>	1	<b>EGFR</b> (Epidermal Growth Factor Receptor)	1M17
	2	<b>KRAS</b> (Kirsten Rat Sarcoma viral oncogene)	4OBE
	3	<b>BRAF</b> (B-Raf Proto-Oncogene)	5VR3
	4	<b>PIK3CA</b> (Phosphatidylinositol 3-Kinase Catalytic Alpha)	7R9V
<b>MAPK Pathway</b>	5	<b>MEK</b>	3EQG
	6	<b>ERK1/2</b>	2ZOQ
<b>Wnt/<math>\beta</math>-Catenin Pathway</b>	7	<b><math>\beta</math>-Catenin</b>	1JDH
	8	<b>GSK-3<math>\beta</math></b> (Glycogen synthase kinase-3 $\beta$ )	1Q41
	9	<b>APC</b> (Adenomatous polyposis coli)	1M5I
<b>PI3K/AKT Pathway</b>	10	<b>PI3K</b> (Phosphoinositide 3-Kinase)	4L2Y
	11	<b>AKT</b> (Protein Kinase B)	1UNQ
	12	<b>mTOR</b> (Mammalian Target of Rapamycin)	4JSN
<b>Novel Protein Biomarkers</b>	13	<b>GREM1</b> (Gremlin-1)	8B7H
	14	<b>CSF2RA</b> (Colony-Stimulating Factor 2 Receptor Alpha)	4RS1

The structural data for each protein was obtained from the Protein Data Bank (PDB) (<https://www.rcsb.org/>), ensuring reliable molecular modeling and docking simulations. These

proteins were chosen based on their high relevance in CRC progression and potential as therapeutic targets, as indicated by prior research studies.

### **2.1.3 Protein Optimization**

To prepare the retrieved protein structures for molecular docking, necessary refinements were performed using Chimera (<https://www.cgl.ucsf.edu/chimera/>). Nonstandard residues, including unwanted ligands, ions, and water molecules, were identified and removed to ensure structural integrity. The cleaned protein structures were then optimized and saved in pdb format for compatibility with subsequent computational studies. Finally, the refined protein files were organized and stored in the designated folder for further docking process.

### **2.1.4. Active Site Identification and Coordinate Extraction**

To facilitate molecular docking, the active sites of the selected proteins were identified by determining their x, y, and z coordinates. This was achieved using DeepSite (<https://open.playmolecule.org/tools/deepsite>), a deep-learning-based tool for binding site prediction. As an alternative approach, PrankWeb (<https://prankweb.cz/>) was also utilized to cross-validate the predicted binding pockets. These tools analyze the protein structure and predict potential ligand-binding sites based on geometric and physicochemical properties. The identified active site coordinates were then used as input parameters for molecular docking studies to ensure accurate and specific ligand interactions.

## **2.2 Ligand Selection and Optimization**

To identify potential drug candidates for repurposing against colorectal cancer (CRC), a systematic screening of FDA-approved drugs was performed using publicly available databases, including DrugBank, ChEMBL, and PubChem. The selection process involved filtering compounds based on their mechanism of action, molecular weight, LogP values, and compliance with Lipinski's rule of five, ensuring drug-likeness and bioavailability.

Since drug repurposing involves identifying existing drugs with potential efficacy against new disease targets, a similarity-based screening was conducted using PubChem. The goal was to identify compounds structurally related to existing anti-cancer drugs but not previously explored for colorectal cancer treatment.

A set of small molecules was selected based on their structural similarity to known anti-cancer agents and their absence from colorectal cancer studies in the literature. The selected

compounds (Table II) were retrieved from PubChem and assessed for their toxicological properties, including hepatotoxicity, immunotoxicity, and cytotoxicity, to ensure potential therapeutic relevance. Literature searches using Google Scholar confirmed that these compounds had not been previously investigated for colorectal cancer, making them viable candidates for further computational analysis.

Table II: Selection of Ligands Based on Similarity to Approved CRC Drugs

Sr. No.	Existing CRC Drug (Approved)	Similar Compound	Database Searched
1.	Adagrasib	Benzimidazole	PubChem
2.		Pyrimidine	PubChem
3.	Regorafenib (Stivarga)	Pazopanib	PubChem
4.		Tivozanib	PubChem
5.	Trifluridine	Fludarabine	PubChem
6.		Vidarabine	PubChem
7.		Brequinar	PubChem

### **2.2.1 Ligand Optimization**

To ensure accurate molecular docking, the selected ligand structures were prepared and optimized using Avogadro (<https://avogadro.cc/>), an open-source molecular editing software. The ligand files in sdf format were imported into Avogadro for processing. Hydrogen atoms were added to satisfy valency requirements, and the molecular geometry was optimized using the Geometry Optimization tool, typically running for 10–15 cycles to achieve a stable conformation. The optimized structures were then saved in mol2 format to ensure compatibility with subsequent docking studies. This preprocessing step helped improve the accuracy of molecular interactions during docking simulations.

## **2.3 Molecular Docking**

### **2.3.1 Protein Preparation**

The selected protein structures were prepared using AutoDock4 (<https://autodock.scripps.edu/>) to ensure compatibility for docking. Initially, the protein structure files in pdb format were loaded into the software. Water molecules were removed to eliminate non-essential solvent interactions, and hydrogen atoms were added to correct atomic valency. Polar hydrogens were merged, and Kollman charges were assigned to account for electrostatic interactions. Finally, AutoDock4 atom types were designated, and the prepared macromolecule was saved in pdbqt format for subsequent docking analysis.

### **2.3.2 Ligand Preparation**

Ligands were prepared using AutoDock, ensuring their chemical structures were optimized for docking. The molecular structures, initially in mol2 format, were imported into AutoDock. The torsion tree was adjusted to define ligand flexibility by making all active bonds non-rotatable. After finalizing the torsional degrees of freedom, the ligands were saved in pdbqt format, making them suitable for docking simulations.

### **2.3.3 Molecular Docking Execution**

Molecular docking was conducted using AutoDock4, following a structured workflow to determine binding affinities between ligands and the target proteins. The docking process commenced with grid box parameter definition, where the binding site coordinates (x, y, z) were obtained using DeepSite and configured within AutoDock. Grid map types were set, and the grid parameter file (GPF) was generated. The AutoGrid4 tool was executed via the command line to calculate affinity maps, preparing the system for docking.

For docking simulations, rigid protein and flexible ligand files in pdbqt format were selected. Genetic Algorithm (GA) based search parameters were employed, optimizing docking accuracy by setting evaluation values to medium. Lamarckian GA was chosen as the docking algorithm. The docking parameter file (DPF) was generated and executed using AutoDock4 via the command line. The results were retrieved in dock.dlg format, containing binding affinities and docking poses for further analysis.

## **2.4 Molecular Dynamics (MD) Simulations**

Molecular dynamics (MD) simulations were conducted to evaluate the structural stability, flexibility, and dynamic behavior of the protein-ligand complex. The simulations were carried out using GROMACS (<https://www.gromacs.org/>), following a structured workflow including system preparation, energy minimization, equilibration, production run, and trajectory analysis.

### **2.4.1 System Preparation**

#### **2.4.1.1 Ligand Preparation for MD simulation**

The ligand was extracted from the protein-ligand complex using Chimera (<https://www.cgl.ucsf.edu/chimera/>). To ensure accurate charge distribution and molecular geometry, hydrogen atoms were added. The ligand structure was then optimized and converted into a compatible format for molecular dynamics simulations. The topology file for the ligand, containing information on atomic interactions, charges, and bonds, was generated using SwissParam (<http://www.swissparam.ch/>).

#### **2.4.1.2 Protein Preparation for MD simulation**

The protein structure was prepared by removing unwanted heteroatoms, ligands, and water molecules. Hydrogen atoms were added to stabilize the protonation state. The CHARMM27 force field was selected to generate the protein topology, ensuring proper atomic interactions and bonded parameters.

#### **2.4.1.3 System Solvation and Neutralization**

To mimic a physiological environment, the protein-ligand complex was placed inside a cubic simulation box with sufficient space around the molecule. The system was solvated using an explicit TIP3P water model. To maintain charge neutrality, counterions were added.

### **2.4.2 Simulation Execution**

#### **2.4.2.1 Energy Minimization**

Before running the MD simulation, energy minimization was performed to remove steric clashes and unstable atomic interactions. This step ensured that the system reached a stable conformation with minimal potential energy.

#### **2.4.2.2 Equilibration**

The system underwent two equilibration steps to achieve stable temperature and pressure conditions:

##### **NVT Ensemble (Constant Number, Volume, and Temperature)**

- The system was equilibrated at a constant temperature while keeping the volume fixed.
- This allowed the molecular system to adapt to the temperature conditions of the simulation.

##### **NPT Ensemble (Constant Number, Pressure, and Temperature)**

- After temperature equilibration, the system was further equilibrated under constant pressure conditions.
- This ensured that the density of the system remained stable, simulating realistic biological conditions.

#### **2.4.2.3 Production Run**

Following equilibration, the final molecular dynamics production run was conducted for 2 nanoseconds (ns) to capture the atomic movements and interactions over time. The trajectory data was recorded at regular intervals for further analysis.

#### **2.4.3 Trajectory Analysis**

After the MD simulation, trajectory analysis was performed to assess the stability and conformational changes in the protein-ligand complex. The following parameters were analyzed:

##### **2.4.3.1 Root Mean Square Deviation (RMSD)**

RMSD was calculated to evaluate structural stability throughout the simulation. A lower fluctuation in RMSD indicates a stable complex, while higher deviations suggest conformational changes.

##### **2.4.3.2 Root Mean Square Fluctuation (RMSF)**

RMSF analysis was conducted to assess the flexibility of individual residues. Higher RMSF values indicate flexible regions, whereas lower values correspond to stable regions of the protein.

#### **2.4.3.2 Radius of Gyration (RoG)**

The RoG was measured to assess the compactness of the protein-ligand complex. A stable RoG value throughout the simulation suggests that the overall structure remained intact, whereas significant variations indicate expansion or collapse of the protein structure.

All graphical analyses, including RMSD, RMSF, and RoG plots, were generated using Matplotlib (<https://matplotlib.org/>) to visualize the molecular behavior over time. The interactions and trajectory visualization were further examined to understand the stability and binding dynamics of the ligand within the active site of the protein.

#### **2.5 ADMET and Drug-Likeness Evaluation**

To assess the pharmacokinetic properties and toxicity profiles of the selected ligands, ADMET (Absorption, Distribution, Metabolism, Excretion, and Toxicity) analysis was performed using **SwissADME** (<https://www.swissadme.ch/>) and **ADMETlab 2.0** (<https://admetmesh.scbdd.com/>). The **SMILES** (Simplified Molecular Input Line Entry System) representation of each ligand was retrieved from **PubChem** (<https://pubchem.ncbi.nlm.nih.gov/>) and used as input for further analysis. SwissADME was utilized to predict drug-likeness properties, including Lipinski's Rule of Five, bioavailability, and gastrointestinal absorption, which are critical for evaluating oral drug potential. Additionally, ADMETlab 2.0 was employed to determine various pharmacokinetic and toxicity parameters, such as hepatotoxicity, clearance, half-life, and blood-brain barrier permeability. The results from these evaluations provided insights into the pharmacokinetic feasibility of the selected compounds and aided in prioritizing potential drug candidates for colorectal cancer treatment.

#### **2.6 Data Visualization**

##### **2.6.1 Visualization of Protein-Ligand Complex**

The interaction between the docked protein-ligand complexes was analysed using Discovery Studio (<https://www.3ds.com/products/biovia/discovery-studio>). The optimized protein-ligand complex was loaded into Discovery Studio to visualize molecular interactions such as hydrogen bonds, hydrophobic interactions, and van der Waals forces. The receptor-ligand interactions were examined, and distance measurements were displayed to assess binding affinity. A 2D interaction diagram was also generated to provide a detailed representation of key binding interactions.

### **2.6.2 Statistical Analysis**

To evaluate docking performance, docking scores of all ligand-protein interactions were compared using heat maps. The heat map was generated using R programming (<https://posit.co/download/rstudio-desktop/>), providing a clear visual representation of binding affinities and aiding in the identification of potential lead compounds.

### **2.6.3 Molecular Dynamics Simulation Analysis**

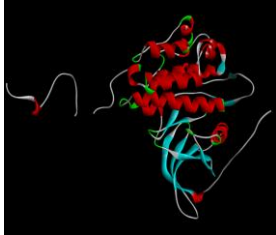
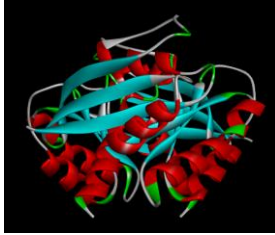
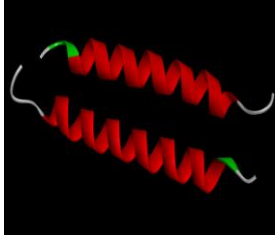
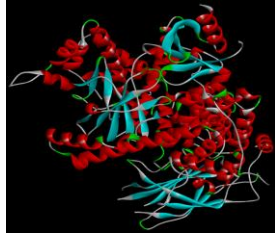
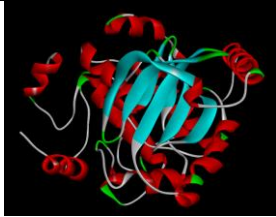

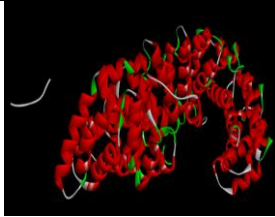
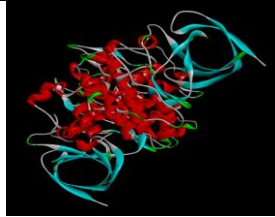
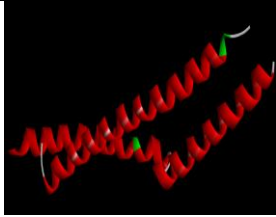
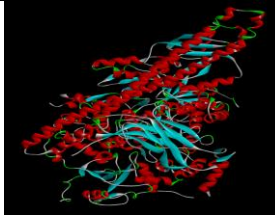
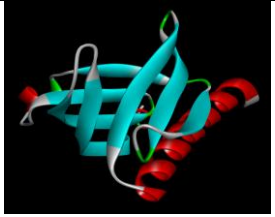
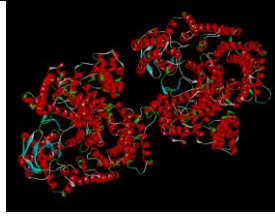
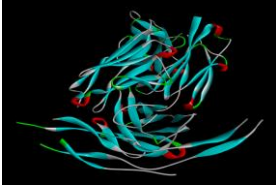

Molecular dynamics (MD) simulations were performed to assess the stability of the protein-ligand complexes over time. The trajectory analysis of MD simulations was carried out using GROMACS tools. Various structural parameters such as root-mean-square deviation (RMSD), root-mean-square fluctuation (RMSF), radius of gyration (Rg) was analyzed. The results were visualized using Matplotlib to better understand the stability and flexibility of the complexes in a dynamic environment.



## RESULTS AND DISCUSSIONS

### 3.1 Structural Analysis of Selected Target Proteins

To visualize the 3D structures of the selected colorectal cancer (CRC) target proteins, their crystallographic structures were retrieved from the Protein Data Bank (PDB). Figure 2-7 represents the 3D structures of the selected proteins, highlighting their overall conformation and molecular architecture.

			
Fig.2: 3D structure of EGFR	Fig.3: 3D structure of KRAS	Fig.4: 3D structure of BRAF	Fig.5: 3D structure of PIK3CA
			
Fig.6: 3D structure of MEK	Fig.7: 3D structure of ERK1	Fig.8: 3D structure of $\beta$ -Catenin	Fig.9: 3D structure of GSK-3 $\beta$
			
Fig.10: 3D structure of APC	Fig.11: 3D structure of PI3K	Fig.12: 3D structure of AKT	Fig.13: 3D structure of mTOR
			
Fig.14: 3D structure of GREM1		Fig.15: 3D structure of CSF2RA	

### 3.2. Identification of Active Sites

The active sites of the selected proteins were identified using DeepSite and PrankWeb, which predict binding pockets based on geometric and physicochemical properties. The validated binding site coordinates (x, y, z) for each protein are presented in Table III.

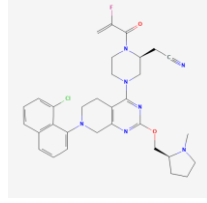
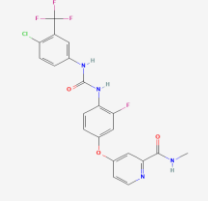
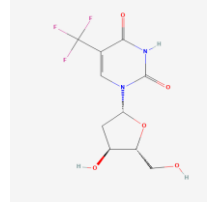
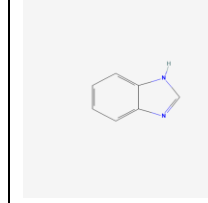
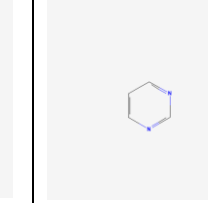
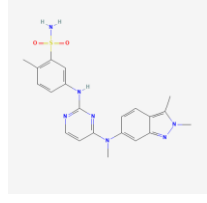
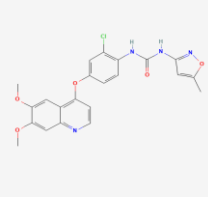
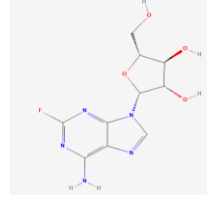
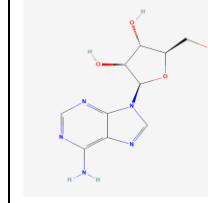
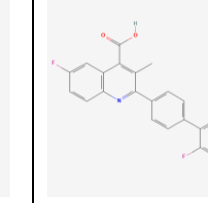
Table III: Active Site Coordinates of Selected Target Proteins

Sr. No.	Protein Name	PDB ID	Active Site Coordinates (x, y, z)
1	EGFR	1M17	(24.79, 2.07, 52.95)
2	KRAS	4OBE	(-20.17, -21.30, 31.02)
3	BRAF	5VR3	(31.19, 16.43, 18.63)
4	PIK3CA	7R9V	(-1.79, -7.88, 11.43)
5	MEK	3EQG	(-4.34, 56.20, 34.04)
6	ERK1	2ZOQ	(0.62, -22.69, 48.61)
7	$\beta$ -Catenin	1JDH	(-3.95, 13.35, 50.56)
8	GSK-3 $\beta$	1Q41	(8.97, -9.86, 14.92)
9	APC	1M5I	(-26.93, 2.25, 22.79)
10	PI3K	4L2Y	(-31.13, 46.63, -42.43)
11	AKT	1UNQ	(27.90, 24.95, 2.0)
12	mTOR	4JSN	(78.54, -21.83, -88.83)
13	GREM1	8B7H	(-7.40, -26.11, 25.67)
14	CSF2RA	4RS1	(22.71, -19.36, -22.88)

### 3.3 Selected Ligands for Drug Repurposing

A set of small molecules was identified through similarity-based screening and drug-likeness evaluation for potential repurposing against colorectal cancer (CRC). The selected compounds were retrieved from PubChem and analyzed for their structural and physicochemical properties.

The 2D structures of these ligands are presented in Figure 16-25.

				
Fig.16: 2D structure of Adagrasib	Fig.17: 2D structure of Regorafenib	Fig.18: 2D structure of Trifluridine	Fig.19: 2D structure of Benzimidazole	Fig.20: 2D structure of Pyrimidine
				
Fig.21: 2D structure of Pazopanib	Fig.22: 2D structure of Tivozanib	Fig.23: 2D structure of Fludarabine	Fig.24: 2D structure of Vidarabine	Fig.25: 2D structure of Brequinar

### 3.4 Molecular Docking Results

#### 3.4.1 Docking Scores of Inhibitors Against Target Proteins

The docking scores of each inhibitor against different target proteins are presented in Table IV and Table V. Lower docking scores (more negative values) indicate better binding affinity.

Table IV: Insilico Docking score of the Compound

	Adagrasib	Regorafenib	Trifluridine	Benzimidazole	Brequinar
AKT	-6.76	-7.04	-4.37	-3.65	-7.00
APC	-5.43	-5.48	-3.58	-3.40	-5.72
BetaCatenin	-5.89	-7.80	-5.24	-4.56	-6.45
BRAF	-6.45	-4.98	-4.23	-3.59	-5.07
CSF2RA	-2.33	-7.55	-5.87	-5.36	-9.11
EGFR	-11.14	-8.55	-6.49	-4.53	-9.47
ERK1	-8.02	-9.25	-5.89	-4.18	-7.98
GREM1	-9.60	-7.55	-4.93	-4.12	-8.18
GSK3Beta	-11.63	-9.56	-5.47	-4.08	-8.89
KRAS	-9.38	-9.13	-5.88	-4.35	-9.12
MEK	-12.03	-9.37	-5.87	-4.91	-8.77
mTOR	-6.98	-6.41	-4.98	-4.79	-5.26
PI3K	-7.72	-8.65	-5.84	-4.88	-9.62
PIK3CA	-9.68	-8.46	-4.81	-3.94	-7.99

Table V: Insilico Docking score of the Compound

	Fludarabine	Pazopanib	Pyrimidine	Tivozanib	Vidarabine
AKT	-5.13	-7.02	-2.85	-6.60	-5.06
APC	-3.68	-5.75	-2.68	-6.52	-3.64
BetaCatenin	-5.98	-8.77	-3.41	-7.73	-6.10
BRAF	-3.90	-5.21	-2.72	-5.79	-3.31
CSF2RA	-5.39	-6.58	-3.45	-8.50	-5.74
EGFR	-6.08	-9.76	-3.22	-9.24	-5.93
ERK1	-4.89	-9.97	-3.12	-8.65	-4.94
GREM1	-4.61	-9.36	-2.86	-7.59	-4.59
GSK3Beta	-5.21	-9.97	-2.90	-8.89	-4.88
KRAS	-5.32	-9.90	-2.93	-9.20	-5.82
MEK	-6.22	-10.94	-3.38	-10.09	-5.52
mTOR	-4.71	-7.53	-2.95	-7.85	-4.50
PI3K	-5.15	-11.72	-3.62	-7.96	-5.11
PIK3CA	-4.68	-8.79	-2.86	-8.00	-4.85

The molecular docking analysis revealed that MEK, EGFR, and PI3K exhibited the strongest binding interactions with multiple inhibitors, suggesting their potential as prime drug targets for colorectal cancer therapy. Among the tested inhibitors, Pazopanib demonstrated the highest binding affinity, particularly for PI3K (-11.72 kcal/mol), ERK1 (-9.97 kcal/mol) and MEK (-10.94 kcal/mol), indicating its strong potential as an effective inhibitor for these key oncogenic pathways. Additionally, Brequinar also showed significant binding interactions, especially with PI3K (-9.62 kcal/mol), EGFR (-9.47 kcal/mol), KRAS (-9.12 kcal/mol) further supporting their role as promising candidates for targeted therapy. In contrast, Pyrimidine exhibited the weakest binding affinity across all target proteins, suggesting limited therapeutic potential and making it a less favorable option for further drug development. These findings emphasize the importance of prioritizing high-affinity inhibitors such as Pazopanib, Brequinar, and Regorafenib (standard molecule) for subsequent validation through molecular dynamics simulations and in vitro studies.

### 3.4.2 Statistical Analysis

To evaluate the binding affinity of the selected inhibitors against key colorectal cancer targets, molecular docking studies were performed. The docking scores (binding energies) indicate the binding between the ligand-target complexes, with lower values signifying stronger binding interactions.

## Heatmap Representation of Docking Binding Affinity

A heatmap visualization (Figure 26) was generated to compare the binding affinities of different inhibitors across multiple target proteins. The colour gradient in the heatmap represents binding energy values, where blue denotes stronger binding (more negative values) and red signifies weaker interactions (fewer negative values).

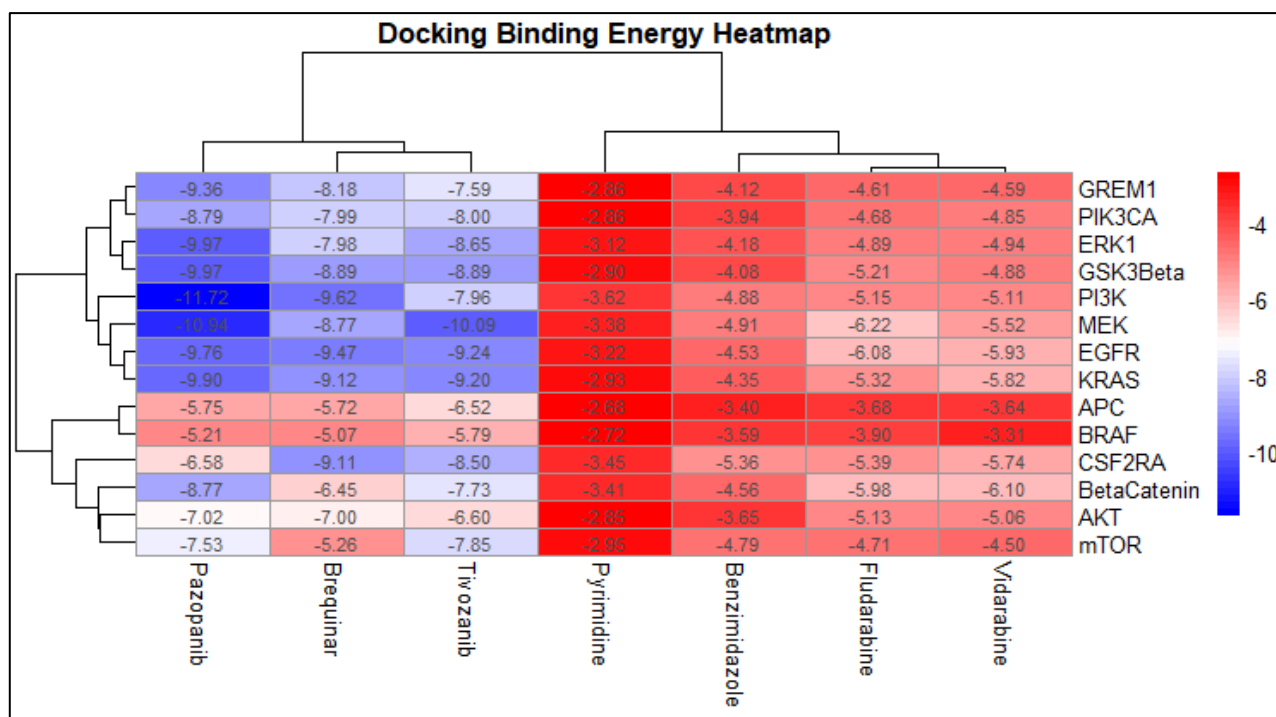


Fig. 26: Heatmap Representation of Molecular Docking Binding Energies

The heatmap analysis provides a visual representation of binding affinities, highlighting key interactions between inhibitors and target proteins. Pazopanib, PI3K, MEK, ERK1 exhibit the strongest binding affinities, as indicated by the deep blue shades, reinforcing their potential as primary targets for colorectal cancer therapy. In contrast, Pyrimidine and Benzimidazole show the weakest binding affinities across most target proteins, suggesting their limited efficacy in inhibiting crucial cancer-related pathways. Among the target proteins, MEK, EGFR, and GSK3Beta stand out due to their strong interactions with multiple inhibitors, indicating their relevance in targeted therapy approaches. Furthermore, KRAS, a well-established oncogenic driver in colorectal cancer, demonstrates moderate to strong binding affinities with most tested compounds, underscoring its significance as a therapeutic target. These observations provide valuable insights into selecting high-affinity inhibitors for further computational and experimental validation.





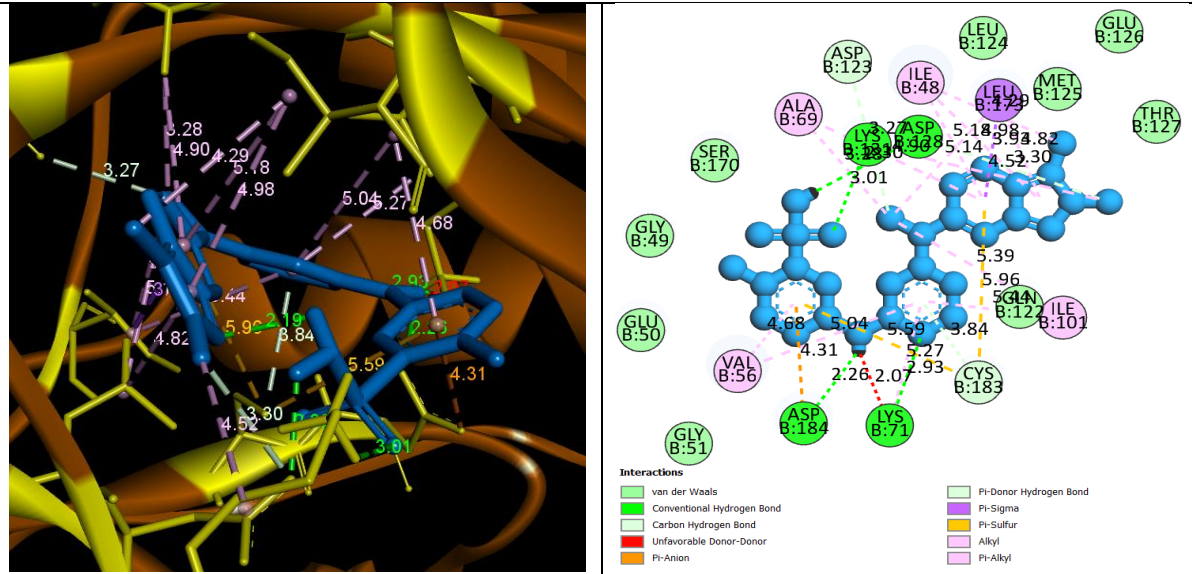


Fig. 29: 3D and 2D structure of Pazopanib with ERK1

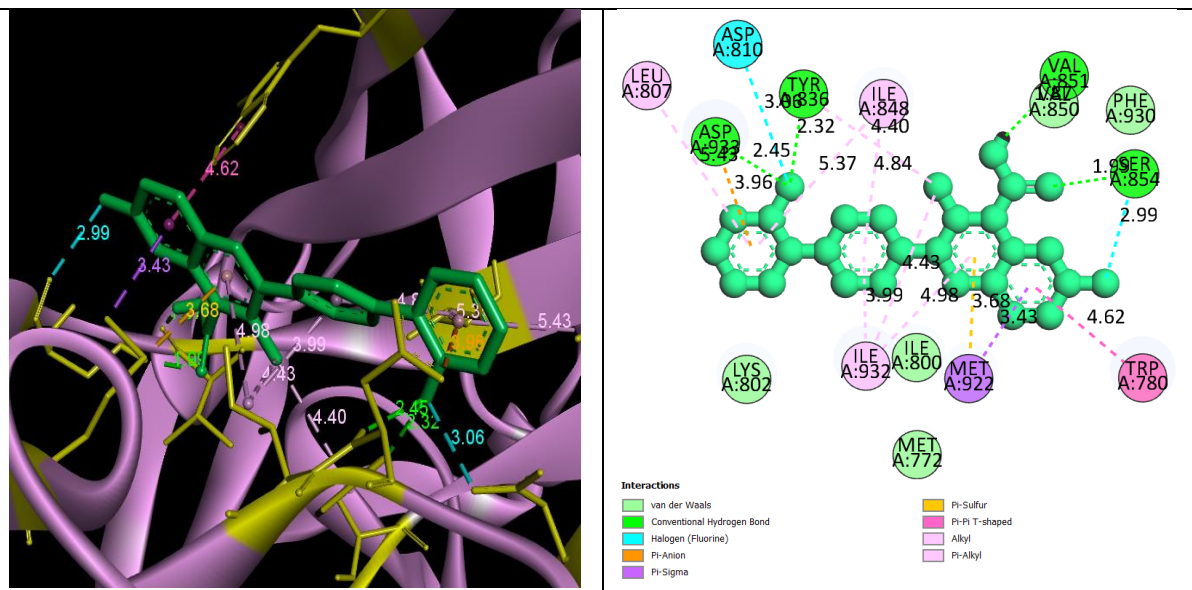


Fig. 30: 3D and 2D structure of Brequinar with PI3K

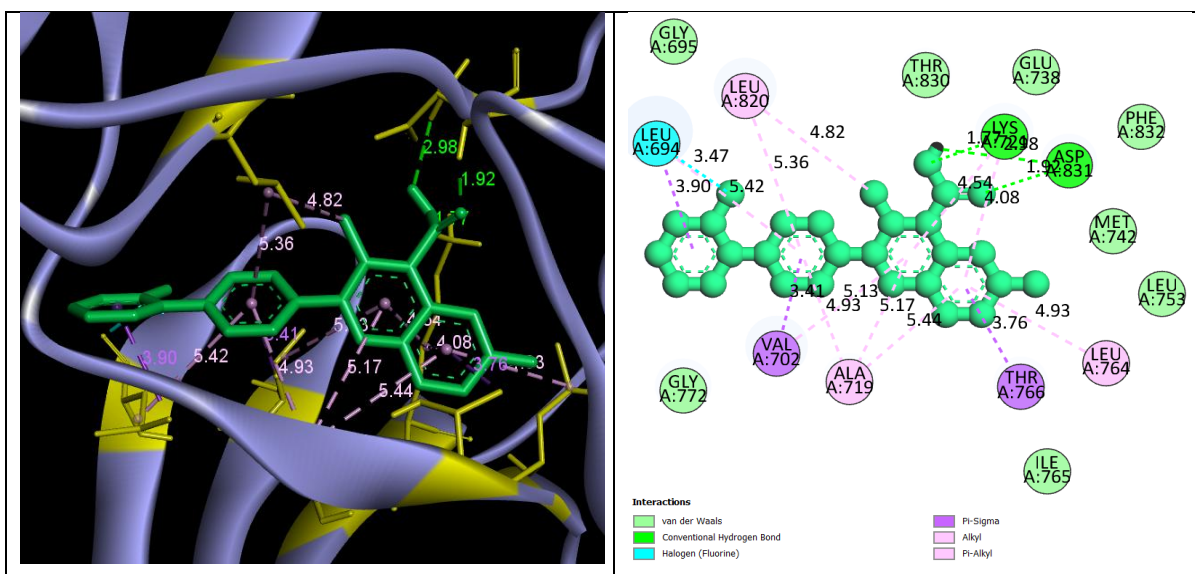


Fig. 31: 3D and 2D structure of Brequinar with EGFR

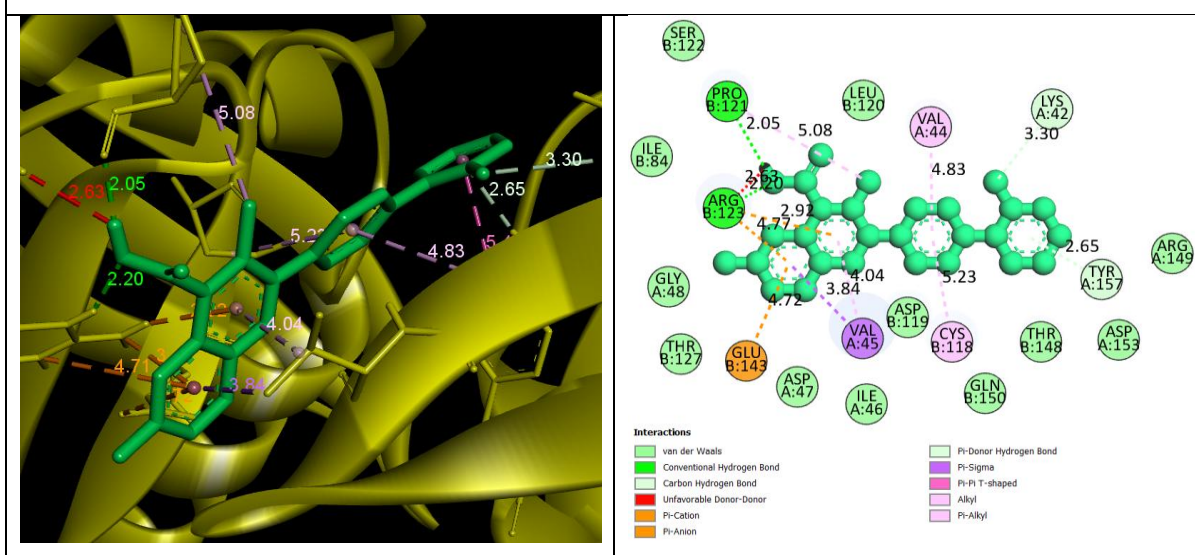


Fig. 32: 3D and 2D structure of Brequinar with KRAS

### 3.6 ADMET and Drug-Likeness Predictions

The success of a drug candidate depends not only on its binding affinity but also on its pharmacokinetic and toxicological properties, which collectively determine its suitability for clinical use. This section evaluates the absorption, distribution, metabolism, excretion, and toxicity (ADMET) properties of the selected compounds along with drug-likeness predictions based on Lipinski's Rule of Five and additional parameters.



Table VI: Structural properties of the Compound

	Adagrasib	Regorafenib	Trifluridine	Benzimidazole	Brequinar
Molar Weight	603.25 g/mol	482.82 g/mol	296.20 g/mol	118.14 g/mol	375.37 g/mol
Num. H-bond acceptors	7	8	8	1	5
Num. H-bond donors	0	3	3	1	1

Table VII: Structural properties of the Compound

	Fludarabine	Pazopanib	Pyrimidine	Tivozanib	Vidarabine
Molar Weight	285.23 g/mol	437.52 g/mol	80.09 g/mol	454.86 g/mol	267.24 g/mol
Num. H-bond acceptors	8	6	2	7	7
Num. H-bond donors	4	2	0	2	4

Adagrasib (603.25 g/mol), Regorafenib (482.82 g/mol), and Trifluridine (296.20 g/mol), the standard drugs already approved for colorectal cancer, exhibit molecular weights within a reasonable range for oral bioavailability, though Adagrasib is slightly above the Lipinski limit. Among the repurposed candidates, Pazopanib (437.52 g/mol) and Brequinar (375.37 g/mol) fall within the optimal range, suggesting good drug-like properties, whereas Tivozanib (454.86 g/mol) is borderline. Benzimidazole (118.14 g/mol) and Pyrimidine (80.09 g/mol) have significantly lower molecular weights, which may enhance permeability but could impact binding efficacy.

Table VIII: Absorption of the Compound

	Adagrasib	Regorafenib	Trifluridine	Benzimidazole	Brequinar
Caco-2 Permeability	-5.31	-5.26	-5.54	-4.35	-4.59
MDCK Permeability	0.0	0.0	0.0	0.0	0.0
Pgp-substrate	Yes	No	No	No	Yes

Table IX: Absorption of the Compound

	Fludarabine	Pazopanib	Pyrimidine	Tivozanib	Vidarabine
Caco-2 Permeability	-5.64	-5.15	-4.29	-4.95	-5.99
MDCK Permeability	0.0	0.0	0.0	0.0	0.0
Pgp-substrate	No	No	No	No	No

The absorption profiles indicate that all compounds exhibit low Caco-2 permeability, suggesting limited passive intestinal absorption. Among them, Pyrimidine (-4.29) and Benzimidazole (-4.35) show relatively better permeability, which may contribute to higher bioavailability. Notably, Adagrasib and Brequinar are identified as P-glycoprotein (Pgp) substrates, implying potential efflux-mediated drug resistance, which can affect therapeutic efficacy. The MDCK permeability values are consistently zero across all compounds, indicating poor permeability through renal epithelial cells.

Table X: Distribution of the Compound

	Adagrasib	Regorafenib	Trifluridine	Benzimidazole	Brequinar
PPB	78.0%	99.2%	48.7%	70.5%	98.6%
VD	2.10	1.57	2.23	0.87	0.37
BBB Penetration	No	No	No	Yes	No

Table XI: Distribution of the Compound

	Fludarabine	Pazopanib	Pyrimidine	Tivozanib	Vidarabine
PPB	30.1%	98.4%	25.7%	98.8%	38.1%
VD	2.15	0.27	0.74	1.07	0.65
BBB Penetration	No	No	No	No	No

Tables X and XII illustrate the distribution properties of the selected compounds. Plasma protein binding (PPB) is notably high for Regorafenib (99.2%), Tivozanib (98.8%), and Brequinar (98.6%), suggesting prolonged circulation and potential reduced free drug availability. In contrast, Trifluridine (48.7%) and Fludarabine (30.1%) exhibit lower PPB, indicating higher free drug concentration in plasma. The volume of distribution (VD) values suggests that Adagrasib (2.10) and Trifluridine (2.23) distribute more extensively in tissues, whereas Pazopanib (0.27) and Brequinar (0.37) remain largely confined to plasma.

Table XII: Metabolism of the Compound

	Adagrasib	Regorafenib	Trifluridine	Benzimidazole	Brequinar
CYP1A2 inhibitor	No	Yes	No	Yes	Yes
CYP2C19 inhibitor	Yes	Yes	No	No	Yes
CYP2C9 inhibitor	Yes	Yes	No	No	No
CYP2D6 inhibitor	Yes	Yes	No	No	No
CYP3A4 inhibitor	Yes	Yes	No	No	No

Table XIII: Metabolism of the Compound

	Fludarabine	Pazopanib	Pyrimidine	Tivozanib	Vidarabine
CYP1A2 inhibitor	No	No	No	Yes	No
CYP2C19 inhibitor	No	No	No	Yes	No
CYP2C9 inhibitor	No	Yes	No	Yes	No
CYP2D6 inhibitor	No	No	No	Yes	No
CYP3A4 inhibitor	No	Yes	No	Yes	No

Tables XII and XIII highlight the metabolism-related properties of the selected compounds, specifically their inhibition of cytochrome P450 (CYP) enzymes. Among the standard colorectal cancer drugs, Regorafenib is a broad-spectrum CYP inhibitor, affecting CYP1A2, CYP2C19, CYP2C9, CYP2D6, and CYP3A4, which may lead to significant drug-drug interactions. Adagrasib also inhibits multiple CYP enzymes, particularly CYP2C19, CYP2C9, CYP2D6, and CYP3A4, indicating a potential for metabolic interactions. In contrast, Trifluridine does not inhibit any CYP enzymes, suggesting a lower risk of metabolic interference.

For the novel compounds, Tivozanib exhibits the highest level of CYP inhibition, affecting CYP1A2, CYP2C19, CYP2C9, CYP2D6, and CYP3A4, similar to Regorafenib, which may impact its metabolism and clearance. Pazopanib also inhibits CYP3A4 and CYP2C9, potentially leading to drug interactions. Benzimidazole and Brequinar show CYP inhibitory activity, particularly against CYP1A2 and CYP2C19, which could influence their biotransformation.

Table XIV: Excretion of the Compound

	Adagrasib	Regorafenib	Trifluridine	Benzimidazole	Brequinar
CL	5.908	2.54	6.45	8.66	0.44
T1/2	0.518	1.51	1.47	2.32	1.63

Table XV: Excretion of the Compound

	Fludarabine	Pazopanib	Pyrimidine	Tivozanib	Vidarabine
CL	10.28	4.38	6.22	0.84	9.25
T <sub>1/2</sub>	2.02	0.54	1.80	1.82	2.03

Tables XIV and XV provide insights into the excretion profiles of the selected compounds, highlighting variations in clearance (CL) and half-life (T<sub>1/2</sub>). Among the standard colorectal cancer drugs, Trifluridine exhibits the highest clearance (6.45 mL/min/kg), indicating rapid elimination, while Regorafenib shows lower clearance (2.54 mL/min/kg) and a longer half-life (1.51 hours), suggesting prolonged systemic retention. Adagrasib, despite its intermediate clearance (5.908 mL/min/kg), has a notably short half-life (0.518 hours), potentially requiring frequent dosing. Among the repurposed candidates, Benzimidazole demonstrates the highest clearance (8.66 mL/min/kg), indicating rapid metabolism, whereas Brequinar has the lowest clearance (0.44 mL/min/kg), suggesting longer retention. Notably, Fludarabine and Vidarabine exhibit both high clearance (10.28 and 9.25 mL/min/kg) and longer half-lives (2.02 and 2.03 hours), which may influence dosing strategies. Tivozanib, with exceptionally low clearance (0.84 mL/min/kg), could provide sustained therapeutic effects.

Table XVI: Toxicity of the Compound

	Adagrasib	Regorafenib	Trifluridine	Benzimidazole	Brequinar
hERG Blockers	0.98	0.56	0.01	0.10	0.33
AMES Toxicity	0.86	0.39	0.52	0.62	0.76
Rat Oral Acute Toxicity	0.99	0.35	0.59	0.56	0.72
Skin Sensitization	0.82	0.13	0.65	0.42	0.05
Carcinogen city	0.81	0.06	0.14	0.57	0.51
Respiratory Toxicity	1.0	0.50	0.72	0.76	0.81

Table XVII: Toxicity of the Compound

	Fludarabine	Pazopanib	Pyrimidine	Tivozanib	Vidarabine
hERG Blockers	0.04	0.59	0.36	0.48	0.02
AMES Toxicity	0.93	0.61	0.09	0.52	0.95
Rat Oral Acute Toxicity	0.15	0.57	0.86	0.33	0.22
Skin Sensitization	0.97	0.00	0.98	0.13	0.98
Carcinogen city	0.62	0.87	0.93	0.77	0.72
Respiratory Toxicity	0.29	0.81	0.95	0.89	0.38

Tables XVI and XVII summarize the toxicity profiles of the compounds, providing key insights into their potential safety concerns. Among the standard colorectal cancer drugs, Adagrasib exhibits high hERG blocking potential (0.98), indicating a higher risk of cardiotoxicity, while Regorafenib and Trifluridine have comparatively lower values (0.56 and 0.01, respectively). Additionally, Adagrasib and Trifluridine show relatively high AMES toxicity (0.86 and 0.52), suggesting potential mutagenic effects. Among the repurposed candidates, Pyrimidine and Vidarabine exhibit minimal hERG inhibition (0.36 and 0.02), indicating a lower risk of cardiotoxicity. However, Pyrimidine has high carcinogenicity (0.93) and AMES toxicity (0.09), raising concerns about its long-term safety. Notably, Pazopanib has a high carcinogenicity risk (0.87), while Tivozanib and Vidarabine show moderate toxicity across different parameters. Respiratory toxicity is notably high for Adagrasib (1.0), Brequinar (0.81), and Tivozanib (0.89), suggesting the need for careful evaluation.

### 3.7 Molecular Dynamics (MD) Simulation Results

#### 3.7.1 Structural Stability Analysis

- **Root Mean Square Deviation (RMSD) Analysis:** Present a graph of RMSD values over simulation time, discussing system stability.

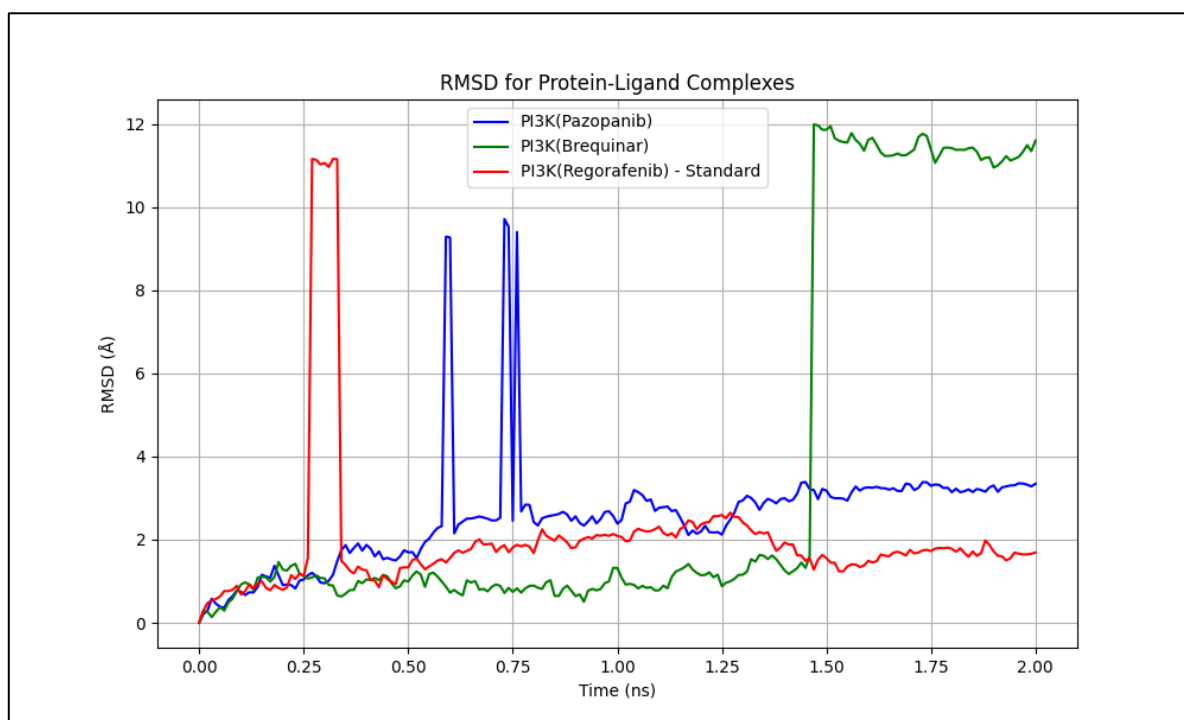


Fig.33: RMSD graph of PI3K with Pazopanib, Brequinar and Regorafenib

The RMSD analysis was performed to compare the stability of drug-repurposed protein-ligand complexes with the standard FDA-approved drug, Regorafenib, in targeting PI3K, EGFR, and KRAS. The PI3K-Regorafenib complex, serving as the standard, exhibited moderate fluctuations initially but stabilized over time, indicating good binding stability. In contrast, PI3K-Pazopanib showed significant fluctuations with high RMSD spikes (Figure 9), indicating poor stability compared to Regorafenib. However, PI3K-Brequinar displayed lower RMSD values, suggesting higher stability than both Pazopanib and Regorafenib, making it a potential alternative for PI3K inhibition.

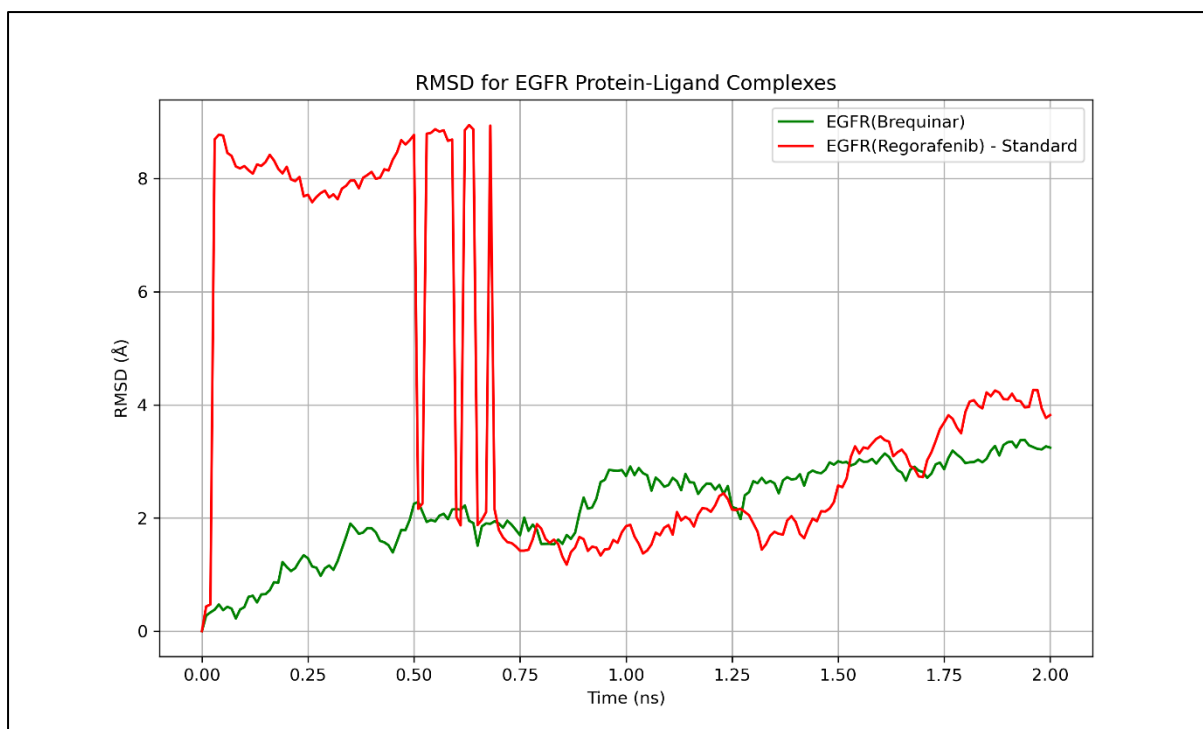


Fig.34: RMSD graph of EGFR with Brequinar and Regorafenib

For EGFR, the standard EGFR-Regorafenib complex stabilized after 1.5 ns, demonstrating moderate stability (Figure 34). The EGFR-Brequinar complex, although initially stable, exhibited slightly higher RMSD values than Regorafenib, indicating lower binding stability.



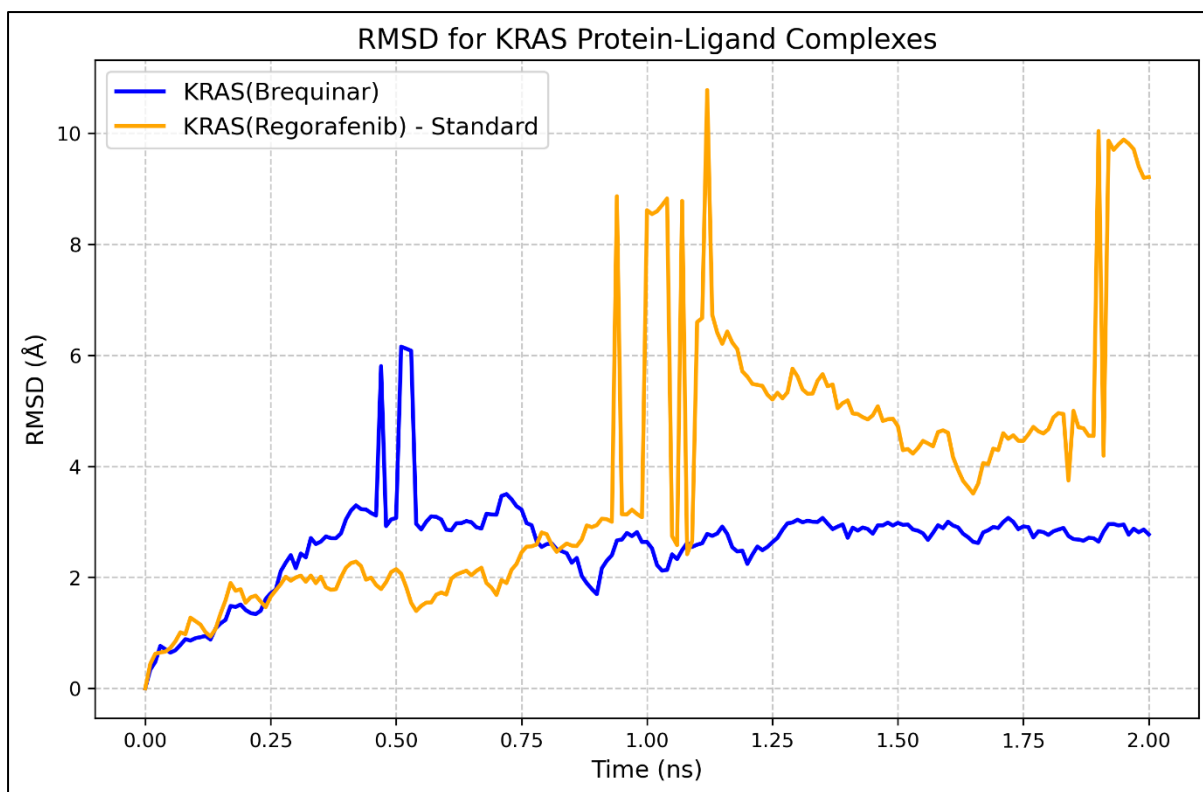


Fig.35: RMSD graph of KRAS with Brequinar and Regorafenib

In the case of KRAS, the standard KRAS-Regorafenib complex showed high fluctuations and instability, indicating weak binding (Figure 35). On the other hand, the KRAS-Brequinar complex maintained relatively lower RMSD values suggesting greater structural stability than Regorafenib.

### 3.7.2 Flexibility and Conformational Analysis

- **Root Mean Square Fluctuation (RMSF) Analysis:** Identify flexible and stable regions within the protein structure.

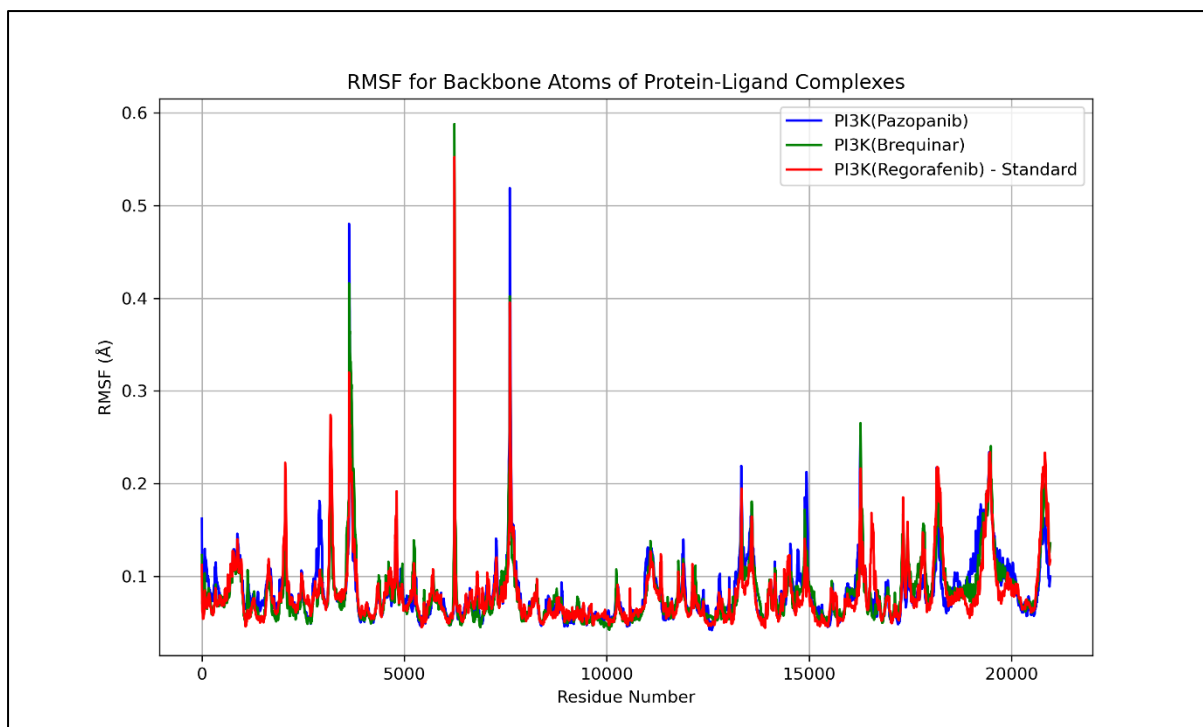


Fig.36: RMSF graph of PI3K with Pazopanib, Brequinar and Regorafenib

The RMSF analysis was conducted to evaluate the flexibility of drug-repurposed protein-ligand complexes in comparison to the standard FDA-approved drug, Regorafenib, for targeting PI3K, EGFR, and KRAS (Figure 36). The PI3K-Regorafenib complex, serving as the standard, exhibited low fluctuations across most residue regions, with RMSF values remaining below 0.2 Å, indicating a relatively stable interaction. The PI3K-Pazopanib complex, however, showed higher fluctuations at multiple residues, suggesting structural instability in certain regions. Conversely, PI3K-Brequinar demonstrated lower RMSF values than both Pazopanib and Regorafenib, implying greater stability and tighter binding to PI3K, making it a promising alternative for inhibition.

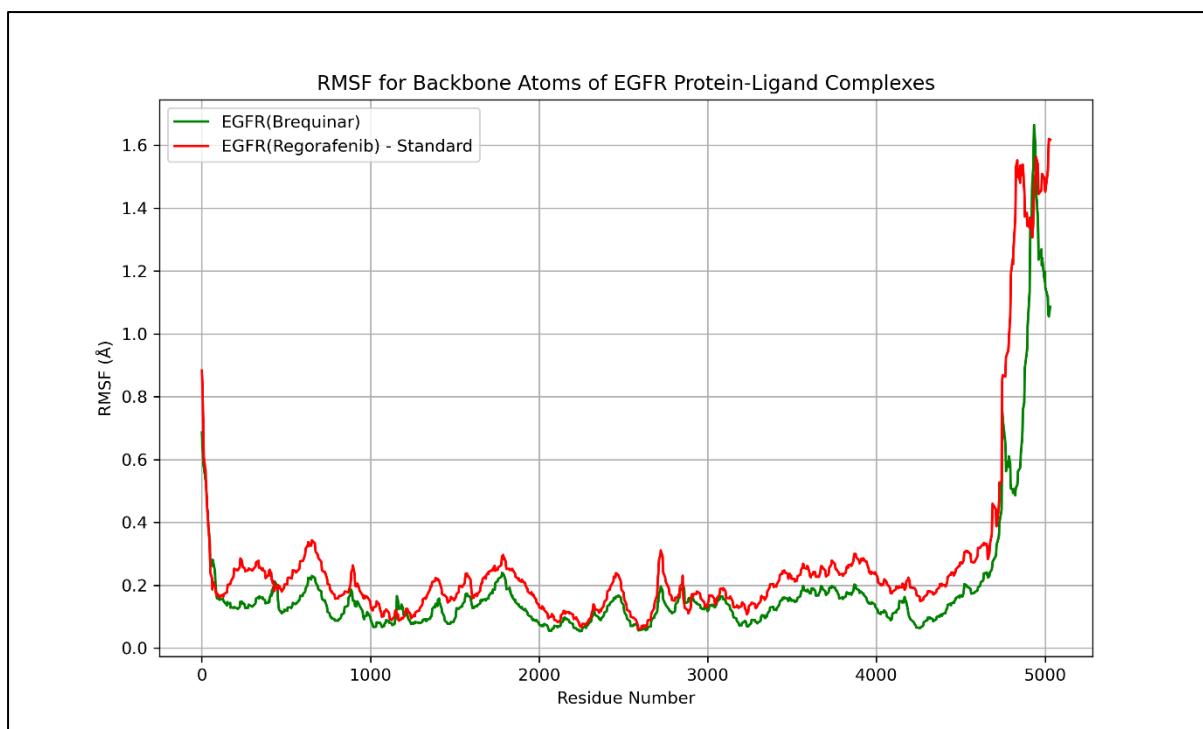


Fig.37: RMSF graph of EGFR with Brequinar and Regorafenib

For EGFR, the standard EGFR-Regorafenib complex exhibited moderate fluctuations, with an increase in RMSF values around highly flexible loop regions (Figure 37). The EGFR-Brequinar complex, while showing a similar trend, displayed higher fluctuations than Regorafenib, suggesting that Brequinar binding induces greater flexibility in certain regions.

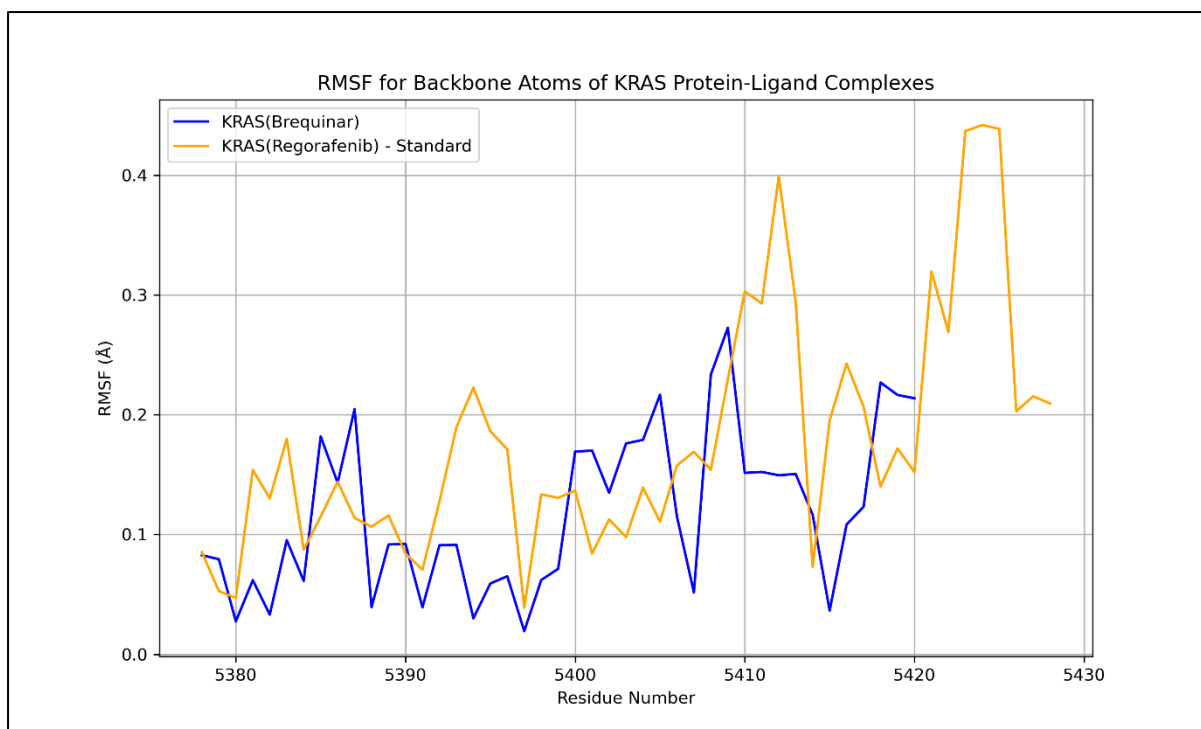


Fig.38: RMSF graph of KRAS with Brequinar and Regorafenib

In the case of KRAS, the KRAS-Regorafenib complex displayed moderate fluctuations, but with a few peaks indicating localized flexibility (Figure 38). However, the KRAS-Brequinar complex exhibited lower RMSF values, suggesting a more stable interaction with KRAS than Regorafenib. This structural stability indicates that Brequinar may provide better inhibition of KRAS.

- **Radius of Gyration (RoG):** Assess the compactness and structural integrity of the protein-ligand complex.

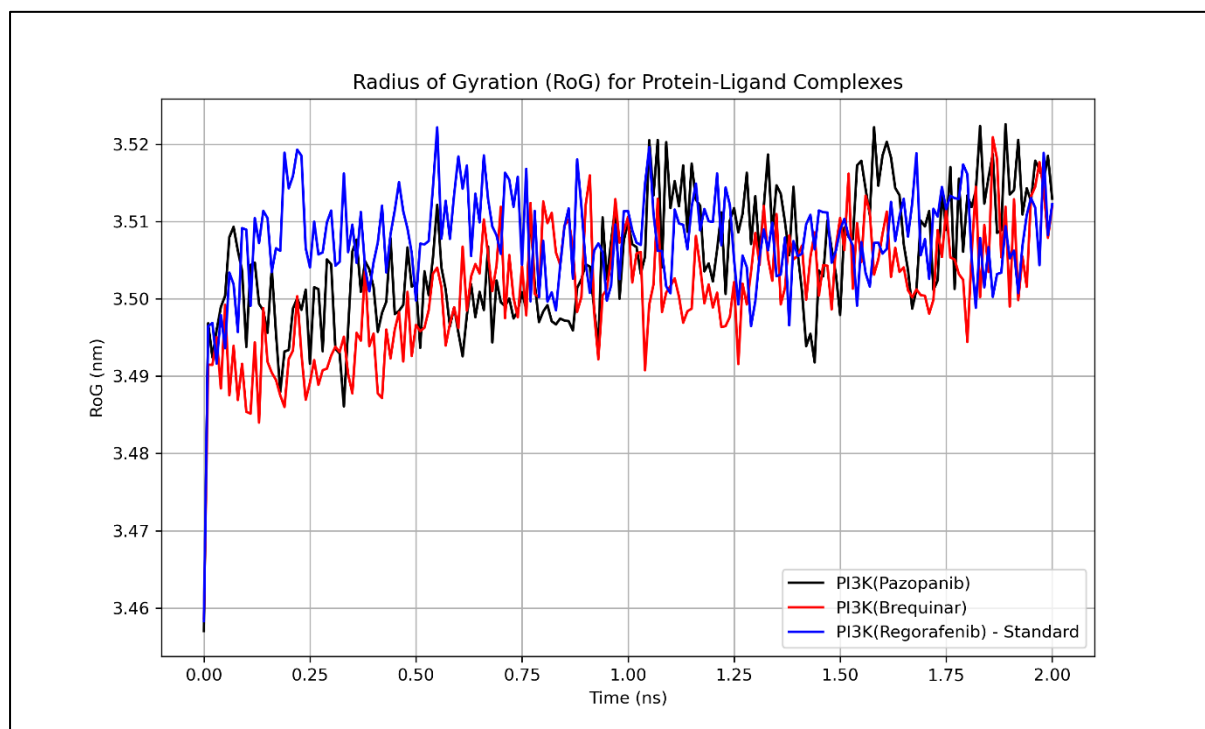


Fig.39: RoG graph of PI3K with Pazopanib, Brequinar and Regorafenib

PI3K complexes (Figure 39), the RoG values for PI3K with Pazopanib (black line), Brequinar (red line), and Regorafenib (blue line) fluctuate between approximately 3.48 and 3.52 nm over the 2 ns simulation. While all three complexes show similar ranges, Regorafenib exhibits slightly less variability and more consistent stability

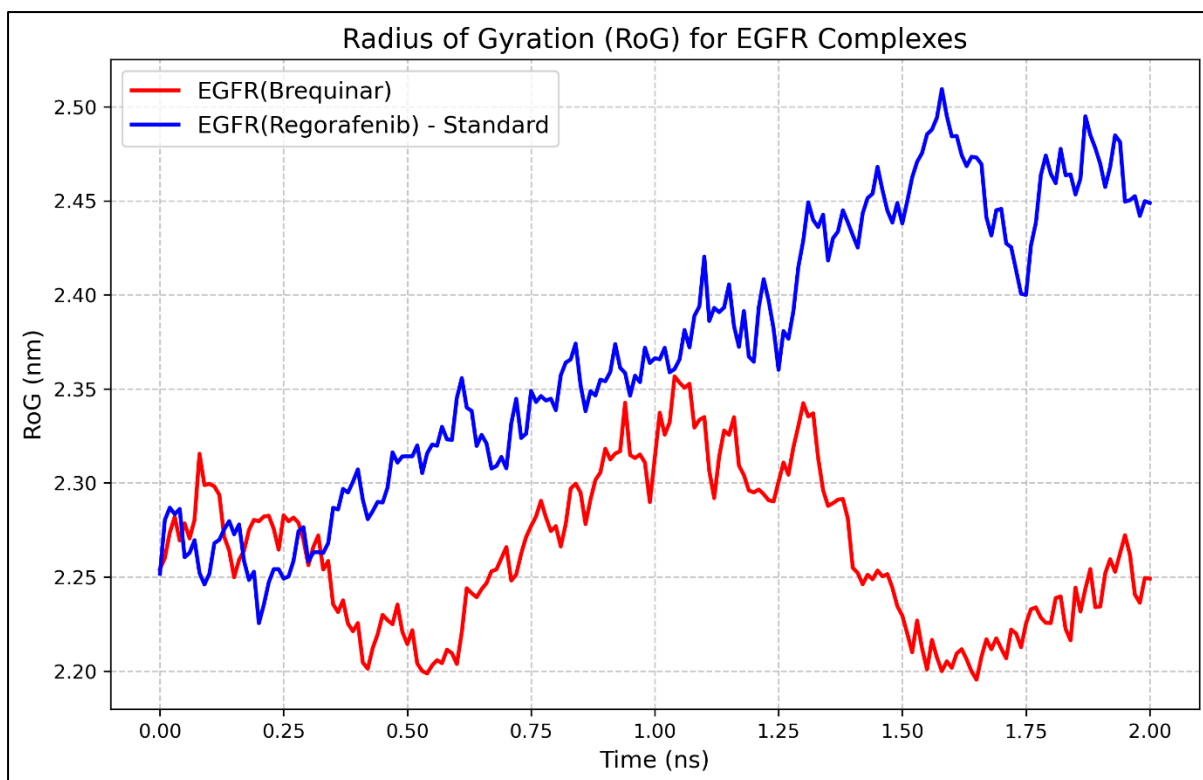


Fig.40: RoG graph of EGFR with Brequinar and Regorafenib

For EGFR complexes (Figure 40), the RoG analysis reveals distinct differences between the repurposed drug Brequinar (red line) and the standard Regorafenib (blue line). Over the 2 ns simulation, both complexes fluctuate between 2.20 and 2.50 nm, but Brequinar shows significant peaks and dips, particularly around 0.5–1.0 ns and later, indicating greater instability and conformational variability.

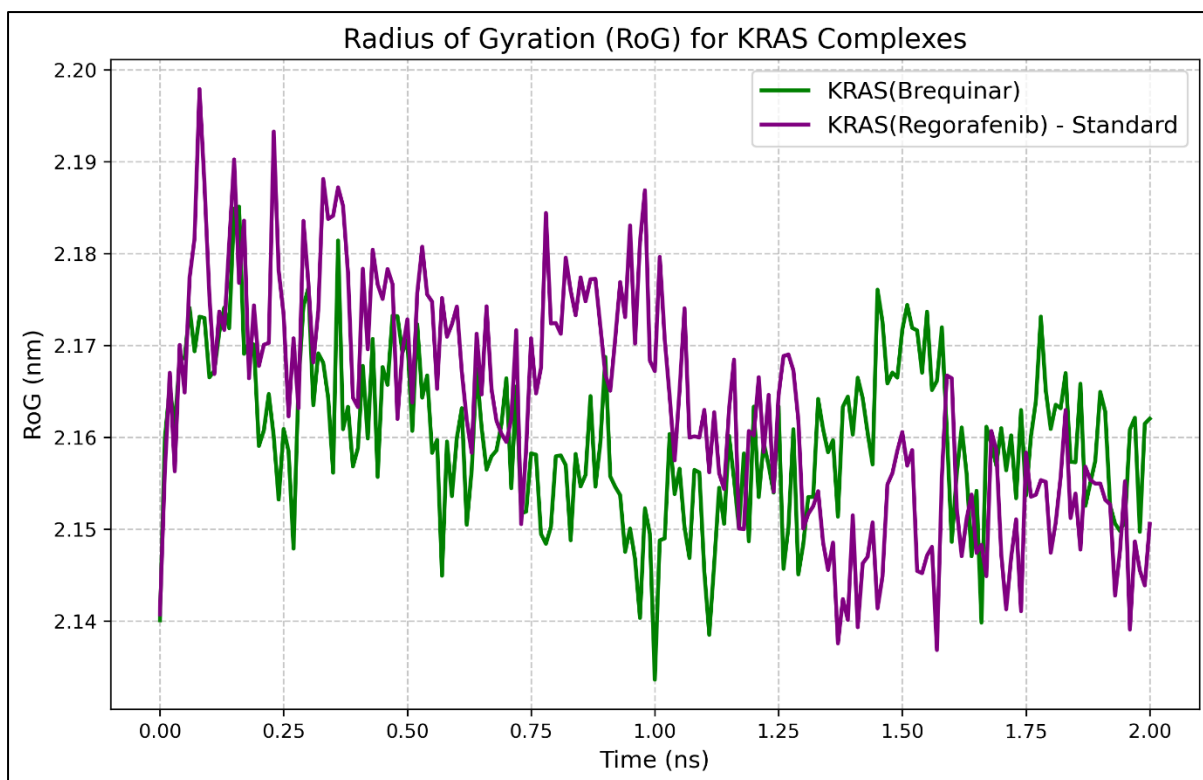


Fig.41: RoG graph of KRAS with Brequinar and Regorafenib

Similarly, the RoG analysis for KRAS complexes (Figure 41) highlights differences between Brequinar (green line) and Regorafenib (purple line), with both fluctuating between 2.14 and 2.20 nm over 2 ns. While Brequinar shows moderate stability with frequent but minor fluctuations, Regorafenib exhibits slightly less variability, particularly after 1.5 ns, indicating better maintenance of compactness and structural integrity.

## 4. Discussion

Colorectal cancer (CRC) is a highly heterogeneous malignancy with complex molecular underpinnings involving multiple dysregulated signalling pathways (Fanelli et al., 2020). The persistent challenges of drug resistance and limited efficacy of current chemotherapeutic agents necessitate the identification of novel therapeutic strategies (Garg et al., 2024). In this study, we explored the repurposing potential of Pazopanib and Brequinar as inhibitors targeting key oncogenic pathways in CRC using a comprehensive *in silico* approach that included molecular docking, ADMET analysis, and drug-likeness evaluation.

Our findings provide valuable insights into the molecular interactions between these drugs and critical CRC-associated targets, including PI3K, MEK, GSK3 $\beta$ , EGFR, and KRAS. The computational evidence presented in this study strongly suggests that Pazopanib and Brequinar exhibit favorable pharmacological profiles and may serve as promising candidates for further preclinical and clinical investigations in CRC therapy.

### 4.1 Interpretation of Results in the Context of Existing Literature

The molecular pathogenesis of CRC is driven by genetic and epigenetic alterations that perturb key signalling cascades, particularly the PI3K/AKT/mTOR, RAS/RAF/MEK/ERK, and Wnt/ $\beta$ -catenin pathways (Schubbert et al., 2007). These pathways regulate essential cellular processes such as proliferation, apoptosis, differentiation, and metastasis. The deregulation of these pathways is associated with therapeutic resistance, making them prime targets for drug development.

Our docking results revealed that Pazopanib and Brequinar exhibit high binding affinities with key CRC-associated proteins, suggesting their potential therapeutic efficacy. Pazopanib, originally developed as a multi-targeted tyrosine kinase inhibitor (TKI) for renal cell carcinoma and soft tissue sarcomas (LaPlant & Louzon, 2010), demonstrated strong interactions with PI3K, MEK, and GSK3 $\beta$ . These targets play a pivotal role in CRC progression, particularly in epithelial-mesenchymal transition (EMT) (Maharati & Moghbeli, 2023) and angiogenesis (He et al., 2021). Previous studies have highlighted that GSK3 $\beta$  inhibition enhances the sensitivity of CRC cells to chemotherapy (Luo, 2009), indicating that Pazopanib might be leveraged to overcome drug resistance.

Brequinar, a potent inhibitor of dihydroorotate dehydrogenase (DHODH) (Madak et al., 2019), was found to strongly bind with PI3K, EGFR, and KRAS. Given that KRAS mutations occur



in approximately 40% of CRC cases (Zhu et al., 2021) and are a primary cause of resistance to EGFR-targeted therapies, Brequinar's interaction with KRAS suggests its potential as a therapeutic alternative for KRAS-mutant CRC. Furthermore, Brequinar has been shown to enhance immunotherapy efficacy (Colligan et al., 2022), which could be explored in combination with immune checkpoint inhibitors for CRC treatment.

Our study aligns with previous research demonstrating the role of small-molecule inhibitors in disrupting these oncogenic pathways. However, our results provide novel insights into the repurposing potential of Pazopanib and Brequinar specifically for CRC, an area that remains underexplored in the existing literature.

#### **4.2 Implications for Drug Repurposing in Colorectal Cancer**

The concept of drug repurposing (or repositioning) has gained considerable traction in oncology due to its cost-effectiveness, reduced timeline for clinical translation, and established safety profiles of FDA-approved drugs (Xia et al., 2024). The ability to repurpose Pazopanib and Brequinar for CRC offers several strategic advantages:

Since both drugs have undergone extensive preclinical and clinical evaluation for other indications, their safety, pharmacokinetics, and dosing regimens are well-characterized. This significantly reduces the time required to advance them into clinical trials for CRC compared to de novo drug development. Given their multi-targeting properties, Pazopanib and Brequinar could be combined with existing CRC therapies such as 5-fluorouracil (5-FU), oxaliplatin, irinotecan, or EGFR inhibitors (cetuximab, panitumumab) to enhance treatment efficacy and overcome resistance mechanisms.

Notably, the inhibition of PI3K, MEK, and KRAS could be particularly beneficial in KRAS-mutant CRC, where conventional EGFR-targeted therapies fail.

Chemoresistance remains a major clinical challenge in CRC treatment (Wang et al., 2024), often driven by PI3K and KRAS mutations. The ability of Pazopanib to target PI3K, MEK and GSK3 $\beta$  and Brequinar's strong interaction with PI3K, KRAS and EGFR suggest that these drugs might reverse resistance mechanisms, improving treatment response rates.

Despite these advantages, it is imperative to validate these findings in preclinical models before progressing to clinical trials. Further studies should evaluate synergistic interactions between these drugs and existing CRC treatments.

## CONCLUSION

Colorectal cancer (CRC) remains a highly heterogeneous malignancy driven by complex molecular alterations, necessitating the development of novel therapeutic strategies. This study explored the potential repurposing of Pazopanib and Brequinar as targeted inhibitors for CRC using an in-silico approach, including molecular docking, molecular dynamics (MD) simulation, ADMET analysis, and drug-likeness evaluation. Our findings indicate that these drugs exhibit strong binding affinities with key CRC-associated proteins, particularly PI3K, MEK, ERK1, EGFR, and KRAS, highlighting their potential therapeutic value.

Pazopanib, a multi-targeted tyrosine kinase inhibitor, demonstrated strong interactions with PI3K, MEK, and ERK1, suggesting its ability to modulate critical pathways involved in CRC progression, epithelial-mesenchymal transition, and angiogenesis. Brequinar, an inhibitor of dihydroorotate dehydrogenase (DHODH), exhibited high affinity for PI3K, EGFR, and KRAS, making it a promising candidate, particularly for KRAS-mutant CRC cases that are resistant to conventional EGFR-targeted therapies. Furthermore, Brequinar's potential role in enhancing immunotherapy efficacy suggests its applicability in combination treatment strategies.

To further assess the stability of drug-protein interactions, we performed a molecular dynamics (MD) simulation for 2 ns. Although research standards typically require 100 ns simulations for comprehensive insights, our 2 ns simulation provided preliminary data indicating the stability and binding efficiency of Pazopanib and Brequinar with CRC-associated proteins.

The repurposing of FDA-approved drugs such as Pazopanib and Brequinar offers significant advantages, including reduced drug development timelines, well-characterized safety profiles, and established pharmacokinetics. These drugs could be integrated into current CRC treatment regimens alongside chemotherapeutic agents like 5-fluorouracil, oxaliplatin, and irinotecan to enhance efficacy and mitigate drug resistance. Given the prevalence of chemoresistance in CRC, targeting PI3K, MEK, and KRAS through these inhibitors may provide a viable strategy for improving treatment response rates.

Despite the promising computational insights, this study has inherent limitations, primarily the lack of extensive experimental validation.

Our study underscores the potential of Pazopanib and Brequinar as promising candidates for CRC therapy. While these findings provide a strong computational foundation, further preclinical and clinical investigations are required to translate these insights into effective

therapeutic applications. The integration of drug repurposing with precision oncology holds promise for enhancing CRC treatment outcomes and addressing current therapeutic challenges.

## FUTURE WORK

While our study provides a strong computational foundation for the repurposing of Pazopanib and Brequinar in CRC, it is not without limitations. The primary constraints of this study are:

The molecular docking and ADMET predictions presented in this study require wet-lab validation. Future studies should include: In vitro assays using CRC cell lines to assess cytotoxicity and apoptosis induction. In vivo models (xenografts, PDX models) to determine pharmacokinetic behavior and tumor suppression efficacy.

While our study provides valuable insights into the potential of Pazopanib and Brequinar as CRC therapeutics through molecular docking and MD simulations, certain limitations must be acknowledged. The MD simulations were conducted for a relatively short duration (2 ns), whereas longer simulations (typically 100 ns) are necessary for a more accurate assessment of drug-protein interaction stability. Future studies should perform extended MD simulations to confirm our findings and gain deeper insights into binding dynamics, conformational changes, and potential allosteric effects.

Although our study provides comprehensive ADMET profiling, further investigations are needed to assess drug metabolism, including CYP enzyme interactions and metabolite formation, potential drug-drug interactions, and transporter-mediated effects such as P-glycoprotein efflux, which are critical for clinical translation. Additionally, given the heterogeneity of colorectal cancer (CRC) and its molecular subtypes (e.g., CMS1–CMS4 classification), Pazopanib and Brequinar may demonstrate varying efficacy across different CRC subtypes. Future research should focus on biomarker-driven patient stratification strategies to optimize personalized therapy and improve treatment outcomes.

## REFERENCES

1. WHO Cancer. Available online: <https://www.who.int/news-room/fact-sheets/detail/cancer>. [(accessed on 08 February 2025)].
2. Ferlay J., Ervik M., Lam F., Colombet M., Mery L., Piñeros M., Znaor A., Soerjomataram I., Bray F. Global Cancer Observatory: Cancer Today. Available online: <https://gco.iarc.fr/today>. [(accessed on 08 February 2025)].
3. U.S. Food and Drug Administration. Step 3: Clinical Research. Available online: <https://www.fda.gov/patients/drug-development-process/step-3-clinical-research>. [(accessed on 09 February 2025)].
4. Li Q., Geng S., Luo H. et al. Signaling pathways involved in colorectal cancer: pathogenesis and targeted therapy. *Sig Transduct Target Ther*, 9, 266, 2024, doi: 10.1038/s41392-024-01953-7.
5. Wang Y., Ji Q., Cao N. et al. CYP19A1 regulates chemoresistance in colorectal cancer through modulation of estrogen biosynthesis and mitochondrial function. *Cancer Metab*, 12, 33, 2024, doi: 10.1186/s40170-024-00360-4.
6. Xia Y., Sun M., Huang H. et al. Drug repurposing for cancer therapy. *Sig Transduct Target Ther*, 9, 92, 2024, doi: 10.1038/s41392-024-01808-1.
7. Garg P., Malhotra J., Kulkarni P., Horne D., Salgia R., Singhal S.S. Emerging Therapeutic Strategies to Overcome Drug Resistance in Cancer Cells. *Cancers*, 16(13), 2478, 2024, doi: 10.3390/cancers16132478.
8. Maharati A., Moghbeli M. PI3K/AKT signaling pathway as a critical regulator of epithelial-mesenchymal transition in colorectal tumor cells. *Cell Commun Signal*, 21, 201, 2023, doi: 10.1186/s12964-023-01225-x.
9. Colligan S.H., Amitrano A.M., Zollo R.A., Peresie J., Kramer E.D., Morreale B., Abrams S.I. et al. Inhibiting the biogenesis of myeloid-derived suppressor cells enhances immunotherapy efficacy against mammary tumor progression. *J Clin Invest*, 132(23), 2022, doi: 10.1172/JCI159167.
10. Hossain M.S., Karuniawati H., Jairoun A.A., Urbi Z., Ooi J., John A., Lim Y.C., Kibria K.M.K., Mohiuddin A.K.M., Ming Ming L.C., Goh K.W., Hadi M.A. Colorectal Cancer: A Review of Carcinogenesis, Global Epidemiology, Current Challenges, Risk Factors, Preventive and Treatment Strategies. *Cancers (Basel)*, 14(7), 1732, 2022, DOI: 10.3390/cancers14071732.

11. Zhu G., Pei L., Xia H. et al. Role of oncogenic KRAS in the prognosis, diagnosis and treatment of colorectal cancer. *Mol Cancer*, 20, 143, 2021, doi: 10.1186/s12943-021-01441-4.
12. He Y., Sun M.M., Zhang G.G. et al. Targeting PI3K/Akt signal transduction for cancer therapy. *Sig Transduct Target Ther*, 6, 425, 2021, doi: 10.1038/s41392-021-00828-5.
13. Castel P., Toska E., Engelman J.A., Scaltriti M. The Present and Future of PI3K Inhibitors for Cancer Therapy. *Nat Cancer*, 2(6), 587-597, 2021, doi: 10.1038/s43018-021-00218-4.
14. Świerczyński M., Szymaszkiewicz A., Fichna J., Zielińska M. New Insights Into Molecular Pathways in Colorectal Cancer: Adiponectin, Interleukin-6 and Opioid Signaling. *Biochim Biophys Acta Rev Cancer*, 1875(1), 188460, 2021, doi: 10.1016/j.bbcan.2020.188460.
15. Ahmad R., Singh J.K., Wunnavu A., Al-Obeed O., Abdulla M., Srivastava S.K. Emerging Trends in Colorectal Cancer: Dysregulated Signaling Pathways (Review). *Int J Mol Med*, 47(3), 1414, 2021, doi: 10.3892/ijmm.2021.4847.
16. Barbosa R., Acevedo L.A., Marmorstein R. The MEK/ERK Network as a Therapeutic Target in Human Cancer. *Mol Cancer Res MCR*, 19(3), 361-374, 2021, doi: 10.1158/1541-7786.MCR-20-0687.
17. Sawicki T., Ruszkowska M., Danielewicz A., Niedźwiedzka E., Arłukowicz T., Przybyłowicz K.E. A Review of Colorectal Cancer in Terms of Epidemiology, Risk Factors, Development, Symptoms and Diagnosis. *Cancers*, 13(9), 2025, 2021, DOI: 10.3390/cancers13092025.
18. ACS Cancer Facts & Figures. 2020. [(accessed on 08 February 2025)]. [Assumed 2020 based on title].
19. Malki A., ElRuz R.A., Gupta I., Allouch A., Vranic S., Al Moustafa A.E. et al. Molecular Mechanisms of Colon Cancer Progression and Metastasis: Recent Insights and Advancements. *Int J Mol Sci*, 22(1), 130, 2020, doi: 10.3390/ijms22010130.
20. Giampieri R., Cantini L., Giglio E., Bittoni A., Lanese A., Crocetti S., Pecci F., Copparoni C., Meletani T., Lenci E., et al. Impact of Polypharmacy for Chronic Ailments in Colon Cancer Patients: A Review Focused on Drug Repurposing. *Cancers*, 12, 2724, 2020, doi: 10.3390/cancers12102724.
21. Jourdan J.P., Bureau R., Rochais C., Dallemagne P. Drug repositioning: A brief overview. *J Pharm Pharmacol*, 72, 1145-1151, 2020, doi: 10.1111/jphp.13273.
22. Kumar S.K., Callander N.S., Adekola K., Anderson L., Baljevic M., Campagnaro E., Castillo J.J., Chandler J.C., Costello C., Efebera Y., et al. Multiple Myeloma, Version

- 3.2021, NCCN Clinical Practice Guidelines in Oncology. J Natl Compr Cancer Netw JNCCN, 18, 1685-1717, 2020, doi: 10.6004/jnccn.2020.0057.
23. Upputuri B., Pallapati M.S., Tarwater P. Thalidomide in the treatment of erythema nodosum leprosum (ENL) in an outpatient setting: A five-year retrospective analysis from a leprosy referral centre in India. PLoS Negl Trop Dis, 14, e0008678, 2020, doi: 10.1371/journal.pntd.0008678.
24. Guo Y., Pan W., Liu S., Shen Z., Xu Y., Hu L. ERK/MAPK signalling pathway and tumorigenesis (Review). Exp Ther Med, 19, 1997-2007, 2020, doi: 10.3892/etm.2020.8454.
25. Bian J., Dannappel M., Wan C., Firestein R. Transcriptional Regulation of Wnt/ $\beta$ -Catenin Pathway in Colorectal Cancer. Cells, 9(9), 2125, 2020, doi: 10.3390/cells9092125.
26. Fanelli G.N., Dal Pozzo C.A., Depetris I. et al. The heterogeneous clinical and pathological landscapes of metastatic Braf-mutated colorectal cancer. Cancer Cell Int, 20, 30, 2020, doi: 10.1186/s12935-020-1117-2.
27. Keum N., Giovannucci E. Global burden of colorectal cancer: Emerging trends, risk factors and prevention strategies. Nat Rev Gastroenterol Hepatol, 16, 713-732, 2019, doi: 10.1038/s41575-019-0189-8.
28. Koveitypour Z., Panahi F., Vakilian M., Peymani M., Seyed Forootan F., Nasr Esfahani M.H., Ghaedi K. Signaling pathways involved in colorectal cancer progression. Cell Biosci, 9, 97, 2019, doi: 10.1186/s13578-019-0361-4.
29. Nowak-Sliwinska P., Scapozza L., Ruiz i Altaba A. Drug repurposing in oncology: Compounds, pathways, phenotypes and computational approaches for colorectal cancer. Biochim Biophys Acta Rev Cancer, 1871, 434-454, 2019, doi: 10.1016/j.bbcan.2019.04.005.
30. Parvathaneni V., Kulkarni N.S., Muth A., Gupta V. Drug repurposing: A promising tool to accelerate the drug discovery process. Drug Discov Today, 24, 2076-2085, 2019, doi: 10.1016/j.drudis.2019.06.014.
31. Narayanankutty A. PI3K/Akt/mTOR Pathway as a Therapeutic Target for Colorectal Cancer: A Review of Preclinical and Clinical Evidence. Curr Drug Targets, 20(12), 1217-1226, 2019, doi: 10.2174/1389450120666190618123846.
32. Madak J.T., Bankhead III A., Cuthbertson C.R., Showalter H.D., Neamati N. Revisiting the role of dihydroorotate dehydrogenase as a therapeutic target for cancer. Pharmacol Ther, 195, 111-131, 2019, doi: 10.1016/j.pharmthera.2018.10.003.

33. Jeong W.J., Ro E.J., Choi K.Y. Interaction Between Wnt/ $\beta$ -Catenin and RAS-ERK Pathways and an Anti-Cancer Strategy Via Degradations of  $\beta$ -Catenin and RAS by Targeting the Wnt/ $\beta$ -Catenin Pathway. *NPJ Precis Oncol*, 2(1), 5, 2018, doi: 10.1038/s41698-018-0049-y.
34. Testa U., Pelosi E., Castelli G. Colorectal cancer: Genetic abnormalities, tumor progression, tumor heterogeneity, clonal evolution and tumor-initiating cells. *Med Sci*, 6, 31, 2018, doi: 10.3390/medsci6020031.
35. Nguyen H.T., Duong H.Q. The molecular characteristics of colorectal cancer: Implications for diagnosis and therapy. *Oncol Lett*, 16, 9-18, 2018, doi: 10.3892/ol.2018.8679.
36. Xue H., Li J., Xie H., Wang Y. Review of Drug Repositioning Approaches and Resources. *Int J Biol Sci*, 14, 1232-1244, 2018, doi: 10.7150/ijbs.24612.
37. Blackadar C.B. Historical review of the causes of cancer. *World J Clin Oncol*, 7, 54-86, 2016, doi: 10.5306/wjco.v7.i1.54.
38. Saletti P., Molinari F., De Dosso S., Frattini M. EGFR Signaling in Colorectal Cancer: A Clinical Perspective. *Gastrointestinal Cancer: Targets Ther*, 5, 21-38, 2015, doi: 10.2147/GICTT.S49002.
39. Papamichael D., Audisio R.A., Glimelius B., de Gramont A., Glynne-Jones R., Haller D., Kohne C.H., Rostoft S., Lemmens V., Mitry E., et al. Treatment of colorectal cancer in older patients: International Society of Geriatric Oncology (SIOG) consensus recommendations 2013. *Ann Oncol Off J Eur Soc Med Oncol*, 26, 463-476, 2015, doi: 10.1093/annonc/mdu253.
40. Deotarse P.J.A., Baile M., Kohle N., Kulkarni A. Drug Repurposing: A Review. *Int J Pharm Res Rev*, 4, 51-58, 2015.
41. Kaya Temiz T., Altun A., Turgut N., Balcı E. Investigation of the Effects of Drugs Effective on PI3K-AKT Signaling Pathway in Colorectal Cancer Alone and in Combination. *Cumhuriyet Med J*, 36(2), 167-177, 2014, doi: 10.7197/1305-0028.33144.
42. Sarkar S., Horn G., Moulton K., Oza A., Byler S., Kokolus S., Longacre M. Cancer development, progression, and therapy: An epigenetic overview. *Int J Mol Sci*, 14, 21087-21113, 2013, doi: 10.3390/ijms141021087.
43. Centelles J.J. General aspects of colorectal cancer. *ISRN Oncol*, 139268, 2012, doi: 10.5402/2012/139268.
44. Idikio H.A. Human cancer classification: A systems biology-based model integrating morphology, cancer stem cells, proteomics, and genomics. *J Cancer*, 2, 107-115, 2011, doi: 10.7150/jca.2.107.



45. Institute of Medicine (US) Forum on Drug Discovery, Development, and Translation. Transforming Clinical Research in the United States: Challenges and Opportunities: Workshop Summary. National Academies Press (US), Washington, DC, 2010.
46. LaPlant K.D., Louzon P.D. Pazopanib: an oral multitargeted tyrosine kinase inhibitor for use in renal cell carcinoma. *Ann Pharmacother*, 44(6), 1054-1060, 2010, doi: 10.1345/aph.1M251.
47. Edwards B.K., Ward E., Kohler B.A., Ehemann C., Zauber A.G., Anderson R.N., Jemal A., Schymura M.J., Lansdorp-Vogelaar I., Seeff L.C., et al. Annual report to the nation on the status of cancer, 1975–2006, featuring colorectal cancer trends and impact of interventions (risk factors, screening, and treatment) to reduce future rates. *Cancer*, 116, 544-573, 2010, doi: 10.1002/cncr.24760.
48. Luo J. Glycogen synthase kinase 3beta (GSK3beta) in tumorigenesis and cancer chemotherapy. *Cancer Lett*, 273(2), 194-200, 2009, doi: 10.1016/j.canlet.2008.05.045.
49. Van Raamsdonk C.D., Bezrookove V., Green G., Bauer J., Gaugler L., O'Brien J.M., Simpson E.M., Barsh G.S., Bastian B.C. Frequent somatic mutations of GNAQ in uveal melanoma and blue naevi. *Nature*, 457, 599-602, 2009, doi: 10.1038/nature07586.
50. Triantafyllidis J.K., Nasioulas G., Kosmidis P.A. Colorectal cancer and inflammatory bowel disease: Epidemiology, risk factors, mechanisms of carcinogenesis and prevention strategies. *Anticancer Res*, 29, 2727-2737, 2009.
51. Schubert S., Shannon K., Bollag G. Hyperactive Ras in developmental disorders and cancer. *Nat Rev Cancer*, 7, 295-308, 2007, doi: 10.1038/nrc2109.
52. Barnett C.F., Machado R.F. Sildenafil in the treatment of pulmonary hypertension. *Vasc Health Risk Manag*, 2, 411-422, 2006, doi: 10.2147/vhrm.2006.2.4.411.
53. Fink H.A., Mac Donald R., Rutks I.R., Nelson D.B., Wilt T.J. Sildenafil for male erectile dysfunction: A systematic review and meta-analysis. *Arch Intern Med*, 162, 1349-1360, 2002, doi: 10.1001/archinte.162.12.1349.
54. Cooper G.M. The Cell: A Molecular Approach. In: The Development and Causes of Cancer. 2nd edition. Sinauer Associates, Sunderland, MA, 2000. Available from: <https://www.ncbi.nlm.nih.gov/books/NBK9839/>.
55. Hanahan D., Weinberg R.A. The hallmarks of cancer. *Cell*, 100, 57-70, 2000, doi: 10.1016/S0092-8674(00)81683-9.
56. Vogelstein B., Fearon E.R., Hamilton S.R., Kern S.E., Preisinger A.C., Leppert M., Nakamura Y., White R., Smits A.M., Bos J.L. Genetic alterations during colorectal-tumor development. *N Engl J Med*, 319, 525-532, 1988, doi: 10.1056/NEJM198809013190901.

57. Doll R., Peto R. The causes of cancer: Quantitative estimates of avoidable risks of cancer in the United States today. *J Natl Cancer Inst*, 66, 1192-1308, 1981.
58. Knudson A.G. Jr. Mutation and cancer: Statistical study of retinoblastoma. *Proc Natl Acad Sci USA*, 68, 820-823, 1971, doi: 10.1073/pnas.68.4.820.
59. Wilson J.M., Jungner Y.G. Principles and practice of mass screening for disease. *Bol Oficina Sanit Panam*, 65, 281-393, 1968.
60. Nordling C.O. A new theory on the cancer-inducing mechanism. *Br J Cancer*, 7, 68-72, 1953, doi: 10.1038/bjc.1953.8.